Hydrological and metabolic controls on dissolved carbon dynamics in groundwater and export to surface waters in a temperate pine forest

Loris Deirmendjian[1], Denis Loustau[2], Laurent Augusto[2], Sébastien Lafont[2], Christophe Chipeaux[2], Dominique Poirier[1], and Gwenaël Abril[1, 3, *].

[1]Laboratoire Environnements et Paléoenvironnements Océaniques et Continentaux (EPOC), CNRS, Université de Bordeaux, Allée Geoffroy Saint-Hilaire, 33615 Pessac Cedex France.
[2]INRA, UMR 1391 Interactions Sol-Plante-Atmosphère (ISPA), 33140 Villenave d'Ornon, France.
[3]Departamento de Geoquímica, Universidade Federal Fluminense, Outeiro São João Batista s/n, 24020015, Niterói, RJ, Brazil.
[*]Now also at Laboratoire d'Océanographie et du Climat, Expérimentations et Approches Numériques (LOCEAN), Centre IRD France-Nord, 32, Avenue Henri Varagnat, F-93143 Bondy, France.

Correspondence to Loris Deirmendjian: lorisdeir@gmail.com

Abstract. We studied the export of dissolved inorganic carbon (DIC) and dissolved organic carbon (DOC) from forested shallow groundwater to first order streams, based on groundwater and surface water sampling and discharge data. In the selected forested and sandy watershed, owing to the very low slope and the high permeability of the soil, hydrology occurs exclusively through drainage of shallow groundwater and no surface runoff occurs. A forest plot on the studied watershed was instrumented for continuous measurements of precipitation, evapotranspiration and net ecosystem exchanges of sensible and latent heat fluxes as well as CO_2 fluxes. Shallow groundwater was sampled at 3 piezometers located in different pines plots, surface waters in 6 first order streams with catchments dominated by pines; and river discharge was modeled based on 4 gauging stations. On a monthly basis and at the plot scale, we found a good consistency between precipitation and the sum of evapotranspiration, shallow groundwater storage and drainage. DOC and DIC stocks in groundwater and exports to first order streams varied drastically during the hydrological cycle, in relation with water table depth and amplitude. In the groundwater, DOC concentrations were maximal in winter when the water table reached the superficial organic-rich layer of the soil. In contrast, DIC in groundwater, which was in majority in the form of excess CO_2, showed maximum concentrations at low water table during late summer, concomitantly with heterotrophic conditions in the forest ecosystem. Our data also suggest that a large part of the DOC mobilized at high water table was mineralized to DIC during the following months within the groundwater itself. In first order streams, DOC and DIC followed a similar seasonal trend as in groundwater but with lower concentrations. On an annual basis, leaching of C to streams occurred as DIC and DOC in similar proportion, but DOC export occurred in majority during short periods of highest water table, whereas DIC export was more constant throughout the year. Leaching of forest C to first order streams represented a small portion (about 2%) of the net land CO_2 sink. In addition, about 65% of the DIC exported from groundwater was not found in streams, as it returned very fast to the atmosphere through CO_2 degassing.

I. **Introduction**

35 Since the beginning of the Industrial Era, human activities have greatly modified the exchange of C between the atmosphere and continents, as well as those occurring along the aquatic continuum that connect the land and the coastal ocean (Ciais et al., 2013; Regnier et al., 2013). Globally, the land (i.e., vegetation and soil) is a major reservoir of C that acts as a net annual C sink (Ciais et al., 2013), and therefore plays a modulator role of the climate system (Heimann and Reichstein, 2008). Within the land, forest ecosystems account for 70% of the storage of all terrestrial plants and 20% of all soil C (Luyssaert et

40 al., 2010), and are consequently important components of the C cycle. Investigate the mechanisms that impact storage and export of C from forest ecosystems is of first interest in both ecosystem and climate researches.

Streams and small rivers are important links between terrestrial and aquatic ecosystems because they receive inputs of C from land and then transform these materials at the land-stream interface and in stream channels as water flows to larger

45 rivers (McClain et al., 2003; Raymond et al., 2013). The C dynamics in forest stream ecosystems results from the interaction between biological activity and retention mechanisms in soils, and water infiltration in soils and drainage (Shibata et al., 2001; Kawasaki et al., 2005). Indeed, biogeochemical cycling within terrestrial ecosystems and across the terrestrial–aquatic interface is dynamically linked with the water cycle (Johnson et al., 2006), because dissolved C is primarily transported by the movement of water (Kawasaki et al., 2005). Furthermore, numerous works in different environments converged to the

50 same conclusion: streams and small rivers are hotspots of CO_2 degassing (Johnson et al., 2008; Butman and Raymond, 2011; Polsenaere and Abril, 2012; Wallin et al., 2013; Kokic et al., 2015). This CO_2 degassing flux results from inputs of groundwater enriched in CO_2 (Hotchkiss et al., 2015), which comes from plant roots respiration and from microbial respiration in soils and groundwater.

55 The quantification of dissolved C fluxes transported by water from terrestrial to aquatic environments is fundamental to resolving the C balance at the catchment scale (Billett et al., 2004; Shibata et al., 2005; Jonsson et al., 2007; Kindler et al., 2011; Dinsmore et al., 2010). Leaching of C from terrestrial ecosystems to streams could potentially represent 40% to 100% of the NEE (i.e., Net Ecosystem Exchange) in a Scotland peat catchment with vegetation consisting of a patchy mix of grasses and sedges (Billett et al., 2004; Dinsmore et al., 2010), 6% in a Sweden boreal catchment dominated by coniferous

60 (Jonsson et al., 2007), on average 6% in five forest plots across Europe (Kindler et al., 2011), and 2% in a Japan temperate catchment dominated by deciduous forest (Shibata et al., 2005). It is important to extend this investigation to other catchments with different landscapes, climatic zones, soil types, vegetation and hydrology, that could considerably improve estimates of C budgets of terrestrial ecosystems.

65 Some authors reported high DIC (Kawasaki et al., 2005; Venkiteswaran et al., 2014) and DOC (Artinger et al., 2000; Baker et al., 2000) concentrations in forested groundwater (i.e., saturated zone). However, estimations of terrestrial C leaching

from direct measurements at the land-water interface (i.e., simultaneously in groundwater and streams) are scarce, which are generally restricted to submarine and coastal environments (Santos et al., 2012; Atkins et al., 2013; Sadat-Noori et al., 2016) and boreal lakes (Einarsdottir et al., 2017), but rarely streams. The few available works that estimates exports of C from land

70   to streams in forested catchments are generally based: (i) on C observations in soil water (i.e., in the unsaturated zone) combined with soil water model that simulates the volume of leached soil water to streams (Öquist et al., 2009; Kindler et al., 2011; Leith et al., 2015), (ii) on differences in the dissolved C flux between upper and lower stream reaches (Shibata et al., 2001, 2005), (iii) on C observations in stream water combined with stream discharge (Dawson et al., 2002; Billett et al., 2004; Dinsmore et al., 2010; Olefeldt et al., 2013), or (iv) as the sum of the three other C fluxes occurring at the scale of a

75   catchment in river systems: CO_2 degassing, organic C burial in sediments and C export downstream (Jonsson et al., 2007). These studies do not enable a complete understanding of the link between C hydrological export and the physical and biological processes occurring in soils and groundwater. In addition, the approaches based on only stream sampling may miss part of the DIC export flux as excess CO_2 that might rapidly degas upstream of the sampling points (Venkiteswaran et al., 2014).

80

In this study, we instrumented a relatively small temperate watershed that offers the convenience of a homogeneous lithology (permeable sandy soil), vegetation (pine forest), topography (very flat coastal plain), as well as a simple hydrological functioning (water outputs mainly as shallow groundwater drainage; there is no surface runoff). The objectives of our study were (i) to investigate the temporal dynamics of dissolved C species in groundwater in relation with

85   hydrological processes in the soil (in particular migration of the water table and groundwater mass balance) and metabolic activity of the forest ecosystem; (ii) to compare spatio-temporal variations of C concentrations in groundwater and first order streams in order to study the fate of dissolved C species at the groundwater-stream interface; (iii) to quantify the leaching of DIC and DOC from groundwater to first order streams in the case of the study site where no surface runoff occurs, based on concentrations of C and discharge data; (iv) to compare this leaching of terrestrial C with net CO_2 exchange of the forest

90   ecosystem and degassing in first order streams.

All the abbreviations used in this paper are listed in table 1.

2. Materials and Methods

2.1. Study site

95   The Leyre watershed (2,100 km²) is located in the southwestern part of France near Bordeaux, in the "Landes de Gascogne" area (Fig. 1). The landscape is a very flat coastal plain with a mean slope lower than 0.125% (generally NW-SE) (Jolivet et al., 2007), but with local gentle slopes (notably near some streams). The mean altitude is lower than 50 m (Fig. 1) (Jolivet et al., 2007). The lithology is relatively homogeneous and constituted of sandy permeable surface layers dating from the Plio-

quaternary period (Legigan, 1979; Bertran et al., 2009, 2011). The soil is composed of sandy permeable podzols characterized by a low pH (4), low nutrient availability, and high organic carbon content that can reach 55 g per kg of soil (Augusto et al., 2010) . There are 3 types of podzols: wet Landes (humic podzol), dry Landes (loose podzol) and mesophyl Landes (duric podzol) (Augusto et al., 2006; Jolivet et al., 2007). The dry Landes, the mesophyl Landes and the wet Landes represents respectively 17%, 36% and 47% of the watershed area (Augusto et al., 2010). Moreover, there is a gradient of soil C from dry Landes (C = 6 to 17 kg m^{-2}) to mesophilic Landes (C = 13 to 30 kg m^{-2}) and wet Landes (C = 15 to 30 kg m^{-2}) (Augusto et al., 2010). The region was a vast wetland until the 19th century, when a wide forest of maritime pine (pinus pinaster) was sown, following landscape drainage from 1850. Nowadays, the catchment is mainly occupied by pine forest (about 80%), with a modest proportion of croplands (about 15%) (Jolivet et al., 2007). The typical rotation period of pine forest is ~40 years, ending in clear-cutting, tilling and re-planting (Kowalski et al., 2003). The climate is oceanic with a mean annual air temperature of 13°C and a mean annual precipitation of 930 mm (Moreaux et al., 2011). Moreover, the average annual evapotranspiration is in the range of 234-570 mm for maritime pine (Govind et al., 2012). Owing to the low slope and the high permeability of the soil (i.e., hydraulic conductivity is about 40 cm h^{-1}, Corbier et al., 2010), the infiltration of rain water is fast (55 cm h^{-1} on average, Vernier and Castro, 2010) and thus surface runoff cannot occur: the excess of rainfall percolates into the soil and fuels the shallow groundwater, rising the water table. Moreover, very low content in feldspars and allover clay minerals in the Leyre sandy podzols induce low water soil retention (Augusto et al., 2010). The sandy permeable surface layers contain a free and continuous water table strongly interconnected with the superficial river network, facilitated by a dense network of drainage ditches, initiated in the 19th century, and currently maintained by forest managers in order to increase trees growth rates (Thivolle-Cazat and Najar, 2001). Furthermore, each type of podzol is characterized with different amplitude of water table depth (Augusto et al., 2006). In the dry Landes of the upper parts of the watershed, as well as near watercourses, the water table is always more than 2 m deep. In the wet Landes of the lower parts, or in the vast interfluves, the groundwater is close to the surface of the soil in winter (0.0-0.5 m depth) and generally remains close to it, even in summer (1.0-1.5 m). The mesophyl Landes corresponds to the intermediate situation. Finally, we adapted the Strahler definition of first order stream by sampling streams and ditches either having no tributaries and/or being seasonally dry.

2.2. Eddy covariance measurements at the forest plot scale

In order to quantify exchanges of carbon and water between the atmosphere and a pine forest plot, we selected the Bilos site (FR-BIL) (Fig. 1) (0.6 km², 44°29'38.08''N, 0°57'21.9''W, altitude: 40 m) that is a quasi-rectangular parcel, owned by the Commune of Salles (France, Gironde) and managed by the National Forest Office. This site is part of the ICOS research infrastructure (http://icos-ri.eu). In December 1999, cutting of the 50 years old forests began with on one quarter of the plot (15 ha) (Kowalski et al., 2003). Following clear-cutting, the site was ploughed to 30 cm depth and fertilized with 60 kg of P_2O_5 per ha in 2001 (Moreaux et al., 2011). In November 2004, the site was divided into two parts, which were seeded with maritime pine (pinus pinaster) with a 1-year lag, in 2004 and 2005, respectively, tree rows being spaced at 4 m (Moreaux et

al., 2011). The site was equipped with an eddy covariance measurement system soon after clearcutting, and the system has been maintained since. The eddy covariance technique allows to determine continuously the exchange between the ecosystem and the atmosphere of sensible heat, CO_2 or H_2O by measuring the turbulent-scale covariance between vertical wind velocity and the scalar concentration of sensible heat, CO_2 or H_2O. The atmospheric exchange originates from atmospheric eddies (turbulence) caused by buoyancy and shear of upward and downward moving air that transport gases such as CO_2 and H_2O.

Here, wind velocity, temperature and CO_2/water vapor fluctuations were measured with, respectively, a sonic anemometer (model R3, Gill instruments Lymington, UK) and an open path dual CO_2/H_2O infrared gas analyzer (model Li7500, LiCor, Lincoln, USA) at the top of a 9.6 m tower (01/01/2014 to 10/05/2014) and with another sonic anemometer (model HS50, Gill instruments) and an enclosed dual CO_2/H_2O infrared gas analyzer (model Li7200, LiCor ©) at the top of a 15 m tower (09/07/14 to 31/12/2015). Consequently, there were no eddy covariance measurements available between 11/05/2014 and 08/07/2014 and thus between these two dates the latent heat fluxes were determined following the procedure of Thornthwaite (1948).

In this paper, raw data were processed following a standard methodology (Aubinet et al., 1999). The post-processing software EddyPro v6.0 (www.licor.com) was used to treat raw data and compute average fluxes (30 min period) by applying the following steps: (1) spike removal in anemometer or gas analyzer data by statistical analysis, (2) coordinating rotation to align coordinate system with the stream lines of the 30 min averages, (3) block average detrending of sonic temperature, H_2O and CO_2 channels (4) determining time lag values for H_2O and CO_2 channels using a cross-correlation procedure, (5) computing mean values, turbulent fluxes and characteristic parameters, and (6) spectral corrections (Ibrom et al., 2007). Thereafter, CO_2 and H_2O fluxes were filtered in order to remove points corresponding to technical problems, meteorological conditions not satisfying eddy correlation theory or data out of realistic bounds. Different statistical tests were applied for this filtering: stationarity and turbulent conditions were tested with the steady state test and the turbulence characteristic test recommended by Kaimal and Finnigan (1994) and Foken and Wichura (1996).

Based on several tests, only values of CO_2 and H_2O fluxes that pass all the filters mentioned above were retained. Then, missing values of CO_2 and H_2O fluxes were gap-filled. The carbon flux (noted NEE) was partitioned into 2 components, GPP (Gross Primary Production) and R_{eco} (Ecosytem respiration) with the R package Reddyproc (version 0.8-2) that implements the procedure of Reichstein et al (2005). During this procedure, NEE was partitioned into GPP and R_{eco} by applying the following steps:

(1) during nighttime GPP = 0 so NEE = R_{eco}

165 (2) statistical regression between R_{eco} and night air temperature and meteorological conditions is adjusted with a Arrhenius type equation (Lloyd and Taylor, 1994) : The width of the adjustment window depends on data availability.

$$R_{eco}=R_{10}(exp[E_0((1/T_{ref}-T_0)-(1/(T_{soil}-T_0))] \qquad (Eq. 1)$$

where,

170 T_{soil} is the soil temperature measured at 10 cm. T_{ref}, R_{10}, E_0 and T_0 are respectively a temperature of 283.15 K, the ecosystem respiration for a reference soil temperature of 10 °C, the activation energy and a calibrated temperature (227.13 K).

(3) day-time R_{eco} is obtained by extrapolating night-time fluxes using the temperature response

(4) GPP is calculated as the difference between daytime NEE and R_{eco}, additional checks are performed to avoid unrealistic

175 values of GPP.

The usual sign convention means that positive NEE indicates an upward flux whereas a negative NEE indicates a downward flux, GPP is positive or zero and R_{eco} is positive. NEE = GPP - R_{eco}.

2.3. Groundwater and surface water monitoring

180 In order to compare groundwater C dynamics at the plot scale and at the watershed scale, we selected 3 piezometers located in different forest types (Fig. 1). According to the depth and amplitude of the water table depth, the three piezometers were representative of dry Landes (Piezometer 2), mesophyll Landes (Piezometer 3) and a situation between mesophyll and wet Landes (Piezometer Bilos). Moreover, the piezometer 2 is located in a riparian mixed pine and oak forest near a first order stream whereas the piezometer 3 is located in another pine forest (approximately same age as Bilos pine forest).

185

We also selected six first order streams whose watersheds were dominated largely with pine forest (~90 %), for the purpose to limit biogeochemical signal from water that have been in contact with croplands.

Shallow groundwater and stream waters were sampled for pCO_2, TA and DOC. The Bilos piezometer was sampled with a
190 frequency of approximately once a month, on 15 occasions between Feb-2014 and Jul-2015 (Tab. S1). In addition, piezometer 2 and 3 were sampled respectively on 11 (Aug. 2014-Jul. 2015) and 6 occasions (Jan. 2015-Jul. 2015) (Tab. S1). The 6 first order streams were sampled on 17 occasions (generally the same day than we sampled piezometers) between Jan. 2014 and Jul. 2015 (Tab. S1).

2.4. Chemical analysis

195 We measured the partial pressure of CO_2 (pCO_2) directly in the field and total alkalinity (TA) and dissolved organic carbon (DOC) back in the laboratory.

Partial pressure of CO_2 in groundwater and streams was measured directly using an equilibrator (Frankignoulle and Borges, 2001; Polsenaere et al., 2013). This equilibrator was connected to an Infra-Red Gas Analyzer (LI-COR®, LI-820), which was calibrated one day before sampling, on two linear segments because of its non-linear response in the range of observed pCO_2 values (0–90,000 ppmv). This non-linearity was due to saturation of the IR cell at pCO_2 values above 20,000 ppmv. We used certified standards (Air Liquide™ France) of 2,079±42; 19,500±390 and 90,200±1,800 ppmv, as well as nitrogen flowing through soda lime for the zero. For the first linear segment [0-20,000 ppmv], which corresponded to river waters, we set the zero and we span the LI-COR at 19,500 ppmv, and we checked for linearity at 2,042 ppmv. For the second segment [20,000-90,000 ppmv], which corresponded to the sampled groundwater, we measured the response of the LICOR with the standard at 90,000 ppmv, and used this measured value to make a post correction of the measured value in the field. For groundwater, we took the precaution to renew the water in the piezometers by pumping of about 300 L with a submersible pump before sampling.

TA was analyzed on filtered samples by automated electro-titration on 50 mL filtered samples with 0.1N HCl as titrant. Equivalence point was determined with a Gran method from pH between 4 and 3. Precision based on replicate analyses was better than ± 5 µM. For samples with a very low pH (<4.5), we bubbled the water with atmospheric air in order to degas CO_2. Consequently, the initial pH increased above the value of 5, and TA titration could be performed (Abril et al., 2015). We calculated dissolved inorganic carbon (DIC) from pCO_2, TA, and temperature measurements (being measured in situ with specific probe Metrhom) using carbonic acid dissociation constants of Millero (1979) and the CO_2 solubility from Weiss (1974) as implemented in the CO_2SYS program (Lewis et al., 1998). Contrary to pCO_2 calculation from pH and TA (Abril et al., 2015), DIC calculation from measured pCO_2 and TA was weakly affected by the presence of organic alkalinity, because 80±20 % of DIC in our samples was dissolved CO_2.

DOC samples were obtained after filtration, in the field through pre-combusted GF/F filters (porosity of 0.7 µm); DOC filtrates were stored in pre-combusted Pyrex vials (25 mL) and acidified with 50 µL of HCl 37 % to reach pH 2 and kept at 4 °C in the laboratory before analysis. DOC concentrations were measured with a SHIMADZU TOC 500 analyzer (in TOC-IC mode), which is based on thermal oxidation after a DIC removal step (Sharp, 1993). The precision (repeatability) was better than 0.1 mg L^{-1}.

2.5. Hydrological monitoring

Precipitation (P) was measured continuously at the Bilos plot using automatic rain gauges with a 30 minutes integration: one Young EML SBS 500 (EML, North Shields, UK) was located in a small clear-cut at 3 m above ground from 01/01/2014 to 10/05/2014 and one electronic gravimetric heated precipitation gauge TRwS (MPS system; Bratislava, Slovakia) was located at the top of the canopy on a 6 m tower, from 01/07/2014 to 31/12/2015. Hence, between 11/05/2014 and 31/06/2014, there

were no P measurements available at the Bilos site. Thus, during this period, we used data from Meteo France © station at Belin-Béliet (about 30 km from the Bilos site). P measurements were also checked weekly in the field with manual reports.

The groundwater table depth (H) was measured continuously at the Bilos plot using high performance level pressure sensors (PDCR/PTX 1830, Druck and CS451451, Campbell Scientific) in one piezometer located amid the Bilos site. The pressure measurements were fully compensated for temperature and air pressure fluctuations. The measurements were obtained at 60 second intervals and integrated on 30 min period. They were checked with manual probe weekly. The groundwater table depth was also measured punctually with a manual piezometric probe in the piezometer 2 and 3 before each groundwater sampling.

Our study took benefit from four calibrated gauging stations of the French water quality agency (with a daily temporal resolution), located on two second order streams (BR and GAR), one third order stream (PL) and one fourth order stream (GL) (Fig.1). We also performed additional discharge measurements in first order streams (Fig. 1). For each stream order, we calculated with a daily temporal resolution for a two years period the drainage (i.e., discharge divided by the corresponding catchment area, in m^3 km^{-2} d^{-1} or in mm d^{-1}) (Deirmendjian and Abril, submitted). We then determined the drainage enrichment α, defined as the ratio between drainage of streams of successive orders. Because of the specific characteristics of the Leyre watershed with no surface runoff, we showed a regular increase in drainage (hence the drainage enrichment α is > 1) between two streams of increasing orders, with drainage enrichment relatively constant temporally. This enabled a precise quantification of additional diffusive groundwater inputs in stream reach compare to that coming from the stream of inferior order. Our analysis leaded to the conclusion that monthly drainage values in first order streams were on average 2.3 times lower than that measured in fourth order stream (Deirmendjian and Abril, submitted).

3. Results

3.1. Water mass balance and hydrological parameters dynamics

We wrote the water mass balance equation at the Bilos forest plot as follows:

P = D + ETR + GWS + ΔS   (Eq. 2)

Where,

P, D, ETR, GWS and ΔS were respectively, precipitation, drainage, evapotranspiration, groundwater storage and change of soil water content in the unsaturated zone, all expressed in mm d^{-1}.

These five parameters were determined respectively as follows:

(1) P was the cumulative precipitation over a given period t as measured at the Bilos site (Fig. 2c);

(2) D was the drainage at the Bilos site; because the flows of the different stream orders were synchronous (Fig. 2a), we estimated D as the mean Leyre River flow over a period t divided by the catchment size at the gauging station and the correction factor of 2.3 due to additional groundwater inputs in reaches of increasing order (Fig. 2c).

(3) ETR was the cumulative evapotranspiration obtained from eddy covariance measurements of latent heat fluxes over a period t at the Bilos site (Fig. 2c).

(4) GWS was the groundwater storage estimated as the net change in water table depth over the period t times the representative soil effective porosity at the Bilos site of 0.2 ((Augusto et al., 2010; Moreaux et al., 2011) (Fig. 2c).

(5) ΔS. No reliable measurements of soil water content were available and this term was not measured therefore. This term was neglected in our water mass balance.

Water mass balance at the Bilos site was calculated on a monthly basis over a two years period (2014-2015) (Tab. 2; Fig. 2c, 3). P on the one hand and the sum of ETR, GWS and D on the other hand closely followed the 1:1 line (Fig. 3), showing the consistency of the water mass balance estimated with different techniques and independent devices.

During the years 2014 and 2015, we distinguished 4 different hydrological periods, HF, GS, LS and EW periods, respectively for high flow, growing season, late summer and early winter periods (Fig. 2). High flow (HF) periods were characterized by two relatively short flood events in Jan. 2014-Mar. 2014 (maximum Leyre river flow of 120 m^3 s^{-1}) and in Feb. 2015-Mar. 2015 (maximum Leyre river flow of 80 m^3 s^{-1}), and associated with high drainage (maximum of 1.9 mm d^{-1} in Feb. 2014) and a water table close to the soil surface (Tab. 2; Fig. 2a-c). High flow periods (HF) were followed by growing season (GS) periods that were associated with decreasing groundwater table (negative groundwater storage), highest evapotranspiration (maximum of 5.3 mm d^{-1} in Apr. 2014) and with both highest GPP and R_{eco} (maximum of 880 and 660 mmol m^{-2} d^{-1}, respectively, in May 2015) in May. 2014-Aug. 2014 and Apr. 2015-Aug. 2015 (Tab. 2, 5; Fig. 2). Growing season (GS) periods were followed by late summer periods (LS) that were characterized with low precipitations (miminum of 0.2 mm d^{-1} in Sep. 2014), and the lowest groundwater table depth in Sept. 2014-Oct. 2014 and in Sep. 2015-Oct-2015 (Tab. 2; Fig. 2a-c). Late summer periods (LS) were followed by early winter (EW) periods that were associated with heavy precipitations (maximum of 4.7 mm d^{-1} in Nov. 2014) and with increasing groundwater table (positive groundwater storage) in Nov. 2014-Jan. 2015 and in Nov. 2015-Dec.2015 (Tab. 2; Fig. 2a-c). We considered that, growing season, late summer and early winter periods, merged together, represented periods of base flow (BF).

Hydrological parameters (i.e., P, D, ETR, GWS) differed considerably between the year 2014 and 2015 (Tab. 2; Fig. 2c). P, D, ETR and GWS were much higher in 2014 (1,102 mm; 912 mm; 191 mm; -72 mm; respectively) than in 2015 (681 mm; 621 mm; 108 mm; -174 mm; respectively) (Tab. 2; Fig. 2c). Evapotranspiration (ETR), precipitation (P) and drainage (D) exhibited strong temporal variabilities (Tab. 2; Fig. 2c). Overall, ETR was higher during high flow and growing season periods (maximum value of 5.3 mm d^{-1} in Apr. 2014) than during late summer and early winter periods (minimum value of

295   0.33 mm d^{-1} in Dec. 2014) (Tab. 2; Fig. 2c). P was higher during early winter and high flow periods (maximum value of 8.0 mm d^{-1} in Jan. 2014) than during growing season and late summer periods (minimum value of 0.2 mm d^{-1} in Sep. 2014) (Tab. 2; Fig 2c). D was mostly impacted by river flow (Fig. 2a-c) and groundwater table depth (H$_m$) (Tab. 3) and therefore was highest during periods of high flow and was lowest during periods of base flow, particularly during late summer (Tab. 2; Fig. 2a-c).

300

Periods for groundwater discharging (decreasing water table) were Feb. 2014-Sep. 2014 and Mar. 2015-Aug. 2015 and these two periods were characterized both by evapotranspiration higher than precipitations and by negative groundwater storage (Fig. 2a-c). Conversely, periods of groundwater loading (rising groundwater table) were Oct. 2014-Feb. 2015 and Sep. 2015-Dec. 2015 and were characterized both by precipitations higher than evapotranspiration and positive groundwater storage

305   (Fig. 2a-c). Consequently, at the plot scale, there was a good linear relationship between groundwater storage and precipitations and between groundwater storage and evapotranspiration (Tab. 3), attesting that evapotranspiration and precipitations played a significant role in the groundwater storage.

3.2. Net Ecosystem exchange of CO$_2$ in the forest plot (Bilos plot)

GPP, R$_{eco}$ and NEE exhibited a strong seasonal variability (Tab. 4; Fig. 2b). GPP. R$_{eco}$ and NEE were respectively 400±220

310   mmol m^{-2} d^{-1}, 310±150 mmol m^{-2} d^{-1} and -90±110 mmol m^{-2} d^{-1} throughout the years 2014 and 2015 (here we excluded 16/05/14-07/07/14 period, because there were no Eddy covariance data available), equivalent to 1,750±960; 1,360±660 and 390±480 g C m^{-2} yr^{-1} (Tab. 4; Fig. 2b). These results were close from Moreaux et al (2011) estimates of 1,720; 1,480 and 340 g C m^{-2} yr^{-1} respectively, as measured at a younger forest stage in the same forest plot. GPP increased from early winter (210±30 mmol m^{-2} d^{-1}) to growing season (640±150 mmol m^{-2} d^{-1}) periods (Tab. 4; Fig. 2b). R$_{eco}$ followed the same temporal

315   trend (Tab. 4; Fig. 2b). During late summer and early winter periods, NEE could be positive (R$_{eco}$>GPP), meaning that the pine forest ecosystems switch from autotrophic to heterotrophic metabolism, notably in Oct. Nov and Dec. 2014, respectively equals to 10, 55 and 20 mmol m^{-2} d^{-1} (Tab. 4; Fig. 2b). NEE was always negative (R$_{eco}$<GPP) during high flow and growing season periods, except for Jul. 2015 (Tab. 4; Fig. 2b) that was probably the consequence of a period of low precipitation (Fig. 2c).

320   ### 3.3. Dissolved carbon evolution in shallow groundwater

In shallow groundwater, TA originated from weathering of silicate minerals with vegetation-derived CO$_2$ (Polsenaere and Abril, 2012). In addition, the proportion of TA in the DIC pool was 5% in shallow groundwater, the large majority of the DIC being composed of dissolved CO$_2$ resulting from microbial and plant root respiration in the soil. This was also consistent with the isotopic signature of the DIC (-26 ‰) and the acidic pH (3-4) in these sampled groundwater

325   (Deirmendjian and Abril, submitted).

One first key result is the opposite temporal evolution of DIC and DOC concentrations in groundwater with water table depth (Tab. 3; Fig. 4). Indeed, DIC and DOC concentrations in groundwater exhibited strong temporal variations in relation with the hydrological cycle (Tab. 5; Fig. 5). On the one hand, during high flow and growing season periods of 2014, the
330   increase of DIC in Bilos groundwater (570 to 3,030 µmol L^{-1}) was associated with both a fast decrease of DOC in Bilos groundwater (3,625 to 950 µmol L^{-1}), in parallel with a decline in the water table (Fig. 5b-c). In 2015, the same temporal trend was observed at the same period, but with a lesser extent (Fig. 5b-c). On the other hand, during period of late summer, the second increase of DIC concentrations in Bilos groundwater (2,700 to 5,400 µmol L^{-1}) was this time not related with any decrease of DOC concentrations in groundwater (Fig. 5b-c). This maximum of DIC concentrations in groundwater
335   corresponded of late summer period where the overlying forest ecosystems switched from autotrophic metabolism to heterotopic metabolism (Fig. 2b). During early winter and high flow periods, DIC concentrations in Bilos groundwater decreased from 4,000 µmol L^{-1} (Nov. 2014) to 1,700 µmol L^{-1} (Mar. 2015), in parallel with a rise in the water table (Fig. 5a-b). Concomitantly, a fast increase in DOC concentrations from 670 to 3,600 µmol L^{-1} occurred in Bilos groundwater between the same time periods (Fig. 5c).

340

DIC concentrations in the three sampled piezometers exhibited a small spatial heterogeneity (Tab. 5; Fig. 5b). DIC concentrations were low (e.g., 570 µmol L^{-1} in the Bilos piezometer in Feb. 2014) during periods of high flow and were high (e.g., 5,370 µmol L^{-1} in the Bilos piezometer in Sep. 2014) during period of late summer (Tab. 5; Fig. 5). In addition, the three sampled groundwater were supersaturated in CO_2 with partial pressure between 7,680 ppmv (during high flow periods)
345   and 116,380 ppmv (during late summer period) (Deirmendjian and Abril, submitted). Alternatively, DOC concentrations exhibited a large spatial heterogeneity, particularly during high flow periods (Tab. 5). During these periods of high flow, DOC concentrations were higher in the Bilos piezometer (3,800±200 µmol L^{-1}) than in the piezometer 2 (280 µmol L^{-1}) and 3 (1,500 µmol L^{-1}) (Tab. 5; Fig. 5c). During the other hydrological periods (periods of base flow), DOC concentrations in the piezometer 2 were still lower than the two other piezometers (Bilos & 3) (Tab. 5). However, during periods of base flow,
350   DOC concentrations in the three sampled groundwater remained more or less constant (Tab. 5; Fig. 5c).

3.4. Dissolved carbon evolution in first order streams

In first order streams, DIC concentrations exhibited smaller temporal variations and significantly lower values that in groundwater, attesting that degassing occurred at the groundwater-stream interface (Tab. 5; Fig. 5b). However, as in groundwater, period of late summer also corresponded to a maximum (1,030±240 µmol L^{-1}) of DIC concentrations in first
355   order streams (Tab. 5; Fig. 5b). First order streams were still supersaturated with CO_2 with values as high as from 3,100 ppmv (during high flow periods) to 27,200 ppmv (during late summer period) (Deirmendjian and Abril, submitted).

In contrast, DOC concentrations in first order streams were in the same order of magnitude than in the piezometer 2, which was located in the dry Landes near a first order stream. However, DOC concentrations in first order streams were lower than in the two other piezometers, which were located in the wet-mesophyl Landes (Bilos) and in the mesophyll Landes
360   (Piezometer 3), in particular during periods of high flow (Tab. 5; Fig. 5c).

As in groundwater, DOC and DIC concentrations in first order streams were negatively correlated (Tab. 3), suggesting that C dynamics in first order streams was mostly impacted by groundwater inputs. Indeed, we observed higher DOC concentrations and lower DIC concentrations in streams during periods of early winter and high flow than during periods of growing season and late summer (Tab. 5).

3.5. Carbon stocks in groundwater and exports to streams

In order to describe quantitatively the dynamics of C at the Bilos plot scale we calculated four different terms: the stocks of DIC (DIC_{stock}) and DOC (DOC_{stock}) in Bilos groundwater (Fig. 6); and the exports of DIC (DIC_{export}) and DOC (DOC_{export}) from Bilos groundwater to first order streams; all integrated between two sampling dates (Tab. S2). The stocks of C in the groundwater can be estimated only for the piezometer Bilos, because we did not have data about the total height of the permeable surface layer in the piezometer 2 and 3. In contrast, because of spatial differences between the dry, mesophyll and wet Landes, the exports of DIC and DOC were calculated for the three study sites (Bilos, piezometers 2 and 3) (Tab. 6).

We wrote:

$$DIC_{stock} = (S_i + S_f) / 2 = (DIC_i \times V_i + DIC_f \times V_f) / 2 \qquad \text{(Eq. 3)}$$

where,

DIC_{stock} was the mean stock of DIC in groundwater between two sampling dates in mmol m². S_f and S_i were the final and the initial stock of DIC in groundwater in mmol m^{-2}. DIC_i and DIC_f were the initial and the final concentration of DIC in groundwater in mmol m^{-3}, respectively. V_i and V_f were the initial and the final volume of groundwater in m^3 m^{-2}.

The volume of groundwater (V) was calculated as the following manner:

$$V = (h + H) \times \Phi_{effective} \qquad \text{(Eq. 4)}$$

where,

h and H (H is negative), were respectively the total height of the permeable surface layer (equals to 10 m, Corbier et al., 2010) and the height of groundwater table. $\Phi_{effective}$ was the effective porosity of the soil and it was equal to 0.2.

Export of DIC in first order streams through drainage of shallow groundwater was calculated using the following equation:

$$DIC_{export} = D \times DIC_m \qquad \text{(Eq. 5)}$$

where,

D and DIC_m were the drainage of shallow groundwater by first order streams and the mean concentration of DIC in groundwater between two sampling dates, respectively in m d^{-1} and mmol m^{-3}.

We calculated DOC$_{stock}$ and DOC$_{export}$ as the same manner.

At the Bilos site, the stocks of DIC and DOC in groundwater followed the same temporal trend than DIC and DOC concentrations (Fig. 5, 6). The stock of DIC increased from high flow (1,140 mmol m^{-2} the 12/02/14) to late summer (8,700 mmol m^{-2} the 24/09/2014) periods, whereas at the same time intervals, the stock of DOC decreased from 7,240 mmol m^{-2} to 780 mmol m^{-2} (Fig. 6). Furthermore, between 12/02/2014 and 16/05/2014 (95 days), we observed an increase of 4,500 mmol m^{-2} in DIC stocks close to the decrease of DOC stocks of 5,500 mmol m^{-2}, suggesting than after the peak of DOC stocks and concentrations at high flow period, groundwater DIC could originates from the degradation of DOC within the groundwater itself. During this period, the degradation rate of DOC in the groundwater was thus estimated of about 60 mmol m^{-2} d^{-1}.

Export of DOC occurred in majority during high flow periods (e.g., 90% of the total DOC export in Bilos plot occurred during high flow periods), for each sampled groundwater (Tab. 6). As observed for DOC concentrations in groundwater, during high flow periods the three sampled groundwater exhibited a large spatial heterogeneity of DOC exports (Tab. 6). During these periods of high flow, DOC export was higher in the Bilos piezometer (3.4±1.1 mmol m^{-2} d^{-1}) than in the piezometer 2 (0.4±0.02 mmol m^{-2} d^{-1}) and 3 (1.5±0.2 mmol m^{-2} d^{-1}) (Tab. 6). These contrasts in DOC exports were related to the water table depth and amplitude (Fig. 4), and the gradient in soil C between the different podzols. In contrast to DOC exports, about the same quantity of DIC was exported during high flow periods (e.g., 50% of the total DIC export in Bilos plot occurred during HF period) than during the other hydrological periods, for each sampled groundwater (Tab. 6). Alternatively to DOC exports, DIC exports, exhibited a smaller spatial heterogeneity between the three sampled groundwater, for each hydrological period (Tab. 6). Finally, although seasonal differences occurred in groundwater between both carbon forms (Tab. 5, Fig. 5b-c), throughout the sampling period, the mean, time-integrated value of carbon export was 0.9±0.5 mmol m^{-2} d^{-1} (3.9±2.4 g C m^{-2} yr^{-1}) for DIC and 0.7±0.7 mmol m^{-2} d^{-1} (2.9±3.0 g C m^{-2} yr^{-1}) for DOC in the three sampled groundwater (Tab. 6). In the Leyre watershed, as drainage of groundwater was the only hydrological pathway, terrestrial C leaching to streams was estimated to be 1.6±0.9 mmol m^{-2} d^{-1} (7.0±3.8 g C m^{-2} yr^{-1}).

3.6. Degassing in first order streams

Because there was no surface runoff in the Leyre watershed we consider that degassing in first order streams (F$_{degass}$) between two sampling dates could be obtained by the difference between pCO$_2$ in groundwater and pCO$_2$ in first order streams as in (Eq. 6).

$$F_{degass} = ((\Delta CO_{2(t)} + \Delta CO_{2(t+1)}) / 2) \times D \qquad \text{(Eq. 6)}$$

where,

$\Delta CO_{2(t)}$ and $\Delta CO_{2(t+1)}$ were the differences between the mean concentrations of CO_2 in mmol m^{-3} in the 3 sampled groundwater and in the 6 first order streams at time t and t+1, expressed in mmol m^{-3}. D is the drainage of the first order streams between time t and t+1 in m d^{-1}.

430

F_{degass} was 0.6±0.3 mmol m^{-2} d^{-1} (2.5±1.3 g C m^{-2} yr^{-1}) throughout the sampling period (Tab. 6). Degassing was more important during periods of high flow than during the other hydrological periods (Tab. 6). In addition, degassing in first order stream was positively correlated to the export of DIC (Tab. 3), suggesting that degassing was mostly impacted by groundwater inputs. Over a hydrological year, 65% of the DIC exported from the three sampled groundwater returned

435 directly in the atmosphere in first order streams through CO_2 degassing (Tab. 6).

4. Discussion

4.1. Water mass balance and the role of groundwater in hydrological export

Our dataset –obtained during an 18 months long monitoring– allows understanding how the water budget is partitioned between the different hydrological parameters (e.g., P, D, ETR and GWS) in the "Landes de Gascogne" area (Tab. 2; Fig. 2c,

440 3). The water budget established at the Bilos plot scale was primarily impacted by precipitation and secondarily by evapotranspiration (Tab. 2; Fig. 2c), as revealed by the annual quantity of precipitation and evapotranspiration (Moreaux et al., 2011).

The transfer of precipitation to rivers involves temporary water storage in groundwater (Oki and Kanae, 2006). The lag time

445 between precipitation and groundwater storage was short at our study site, as attested by the strong linear relationship between these two parameters (Tab. 3). Thus, when precipitations are high (during early winter and high flow periods), water infiltration in the sandy podzols is faster than the capture by vegetation. Consequently, groundwater is filled directly by rain water infiltration, which raises the water table and thus increases the groundwater storage (Fig. 2a-c). This is consistent with the sandy texture of soils with a high proportion of coarse sands (Augusto et al., 2010), which makes the infiltration of rain

450 water fast (Vernier and Castro, 2010). In addition, the correlation between groundwater storage and precipitation is also consistent with findings of Alley et al. (2002) who highlight that groundwater recharge can occur as a result of precipitation over large areas, infiltrating and percolating through the unsaturated zone in regions having shallow groundwater table.

On the contrary, the transpiration flow through plants and the evapotranspiration were maximum during growing season and

455 late summer periods when the precipitations were low (Tab. 2, Fig. 2c). For that reason, the groundwater storage decreases with increasing evapotranspiration (Tab. 3; Fig. 2c), revealing that soil water and water table uptake by the pine trees directly lowers the water table. This is consistent with reports of Vincke and Thiry (2008) who found that water table uptake contributes to 60% of the evapotranspiration for an experimental Scots Pine plot in a flat and sandy area of Belgium, which process occurred through capillary rise from the groundwater up to the rooted soil layers. Furthermore, groundwater table

460 uptake has been also observed for deciduous trees (cork oak trees) (Mendes et al., 2016), and associated this time with a dimorphic root system which allows the access and use of groundwater resources (David et al., 2013). The positive correlation between groundwater storage and evapotranspiration is also consistent with a water table more elevated after harvesting pine forest due to reduced evapotranspiration (Bosch and Hewlett, 1982; Sun et al., 2000; Xu et al., 2002). In the "Landes de Gascogne" area, drainage significantly increased in clear cut areas due to reduced evapotranspiration, (Kowalski

465 et al., 2003; Loustau and Guillot, 2009). Indeed, the network of drainage ditches created by foresters evacuates very rapidly the water in excess when the groundwater level rises. Since most pine roots are located in the first meter of the soil (Bakker et al., 2006), to avoid winter anoxia caused by rising water table (Bakker et al., 2006, 2009), the pine trees do not exhibit any transpiration reduction when the groundwater is high (Loustau et al., 1990).

470 We observed a lag time between groundwater storage and drainage at our study site (Fig. 2a-c, 3), as attested by the nonlinear relationship between these two parameters (Tab. 3). This lag time effect was due to the time of water travel in groundwater, depending on the spatial temporal gradient of hydraulic head, hydraulic conductivity, and porosity of the system (Alley et al., 2002; Ahuja et al., 2010). At our study site, shallow groundwater acts as a buffer, the drainage being mostly controlled by water table depth and the capacity of the porous soil to store or export water (Alley et al., 2002). This is

475 consistent with Vissers and van der Perk (2008) who highlight that groundwater flow of a shallow sandy aquifer is largely controlled by the drainage pattern of the streams and ditches, and thus by the water table depth and topography of the area. At our study site, the buffer capacity of groundwater induces regional hydrological characteristics; (i) the river discharge increased at period of high flows, while high precipitation and rising water table started in early winter 2-3 months before (Fig. 2a-c); (ii) the river discharge remained relatively constant between periods of late summer and early winter, although

480 the water table was rising (Fig. 2a-c). In the Leyre watershed, sudden hydrological events are thus buffered by this temporary groundwater storage in the porous soil. As a consequence, at our study site, temporary groundwater storage mediates all the C exports to the watershed. Moreover, storms would not have such crucial impact on the way we estimate C stocks and exports from groundwater, based on monthly sampling frequency. Indeed, with our monthly resolution we could appreciate the seasonal effect of DIC and DOC in shallow groundwater and streams (Fig. 5b-c), suggesting that the main processes that

485 impact C dynamics in groundwater and streams were taking into account. On the contrary, in other types of catchments (e.g., steeper and less permeable), C stocks and exports are quickly affected by storms or pulsed hydrological events (e.g., Raymond and Saiers, 2010; Wilson et al., 2013). Finally, the water mass balance at the Bilos plot scale being consistent with drainage modeled and estimated at the watershed scale (Fig. 2c, 3), we used this drainage in the purpose of estimate C exports at the plot scale (Tab. 6).

490 **4.2. Soil carbon leaching to groundwater**

Generally, dissolved organic matter includes a small proportion of identifiable, low molecular weight compounds such as carbohydrates and amino acids and a larger proportion of complex, high molecular weight compounds (Evans et al., 2005; Kawasaki et al., 2005), such as in our study region (Delprat, 1997). DOC in soil and river water originates from biological

decomposition of dissolved organic matter, throughfall or litter leaching, root exudates (Bolan et al., 2011). Surface precipitation generally drives the transport of DOC through the soil column to the saturated zone (Kawasaki et al., 2005; Shen et al., 2015). In the sandy podzols of the Landes de Gascogne, soil DOC in upper horizons was not preferentially mobilized by rainwater percolation, as revealed by the relative stability of DOC concentrations and stocks in groundwater during periods of base flow, i.e. when groundwater table was low and the surface soil was drained (Tab. 5; Fig. 5c). Indeed, up to 90% of surface-derived DOC can be removed prior to reaching the saturated zone (Shen et al., 2015). This suggests the occurrence of retention mechanisms in soils during vertical infiltration that strongly impact DOC leaching from soil to groundwater (Kawasaki et al., 2005; Shen et al., 2015). As a matter of fact, a large fraction of DOC in soil solution is sorbed onto soil minerals or metal as it moves downward rather than mineralized by soil microorganisms (Kaiser and Guggenberger, 2000; Sanderman and Amundson, 2009). Sandy podzols contain almost no clay minerals (Augusto et al., 2010), and this absence of phyllosilicates likely prevents the formation of DOC-clay complex from occurring, and thus retention in soil is probably more influenced by DOC-metal complex. Indeed, organometallic associations play a key role in the development of podzols (Lundström et al., 2000a; Lundström et al., 2000b; Sauer et al., 2007). In temperate forested ecosystems, Michalzik et al (2001) and Kindler et al (2011) evidenced that leaching of DOC from subsoils was controlled by retention in the mineral B horizon of the soil, this retention being related with the content of extractable aluminum and iron oxides in the soil (Kindler et al., 2011). These Al-Fe oxides are considered to be the most important sorbents for dissolved organic matter in soils (e.g., Kaiser et al., 1996). In podzols, the content in Al-Fe oxides, and their degree of complexation by soil organic matter, increased with depth (Ferro-Vázquez et al., 2014), such as our study site (Achat et al., 2011). Furthermore, where sorptive retention of DOC occurs, it contributes to carbon accumulation in subsoils due to the stabilization of organic matter against biological degradation (Kalbitz and Kaiser, 2008). The sorption processes being affected by molecular properties such as size, hydrophobicity and charge (Inamdar et al., 2012). At our study site, the fraction of groundwater DOC that predominates at low water table was probably more recalcitrant, more stabilized and more aged. Indeed, in a small forested temperate basin, Schiff et al (1997) reported a wide range of ^{14}C age of groundwater DOC, from old DOC at base flow under dry conditions to relative modern DOC during high flow or wetter conditions. At our study site, during these low water table periods, groundwater DOC was on average higher at at the mesophyl to wet Landes station (Bilos and Piezometer 3), than at the dry Landes (Piezometer 2) (Tab. 5). Several studies have reported decreasing DOC concentrations in groundwater in concurrence with increasing subsoil thickness and water table depth (Pabich et al., 2001; Datry et al., 2004; Goldscheider et al., 2006), with DOC concentrations at or close to zero reported in deep (> 1 km) and old groundwater (Pabich et al., 2001). The transfer of DOC in groundwater also depending on the level of hydraulic connectivity between subsoils horizons and water table depth (Kalbitz et al., 2000). At our study site, the saturation of the superficial organic-rich horizon of the soil is necessary to generate high DOC concentrations in groundwater (Fig. 4, 5, 7). Under reducing conditions in soils, as during periods of high flow at our study site, the dissolution of Fe oxides in soil increases not only dissolved Fe concentrations but also DOC concentrations, as a consequence of the diminished sorptive retention of DOC (Hagedorn et al., 2000; Camino-Serrano et al., 2014; Fang et al., 2016). Furthermore, we calculated a stock of soil

organic C in the 0-60 cm layer of 9.7 kg m^{-2} at the Bilos plot (Trichet and Loustau, personal communication), whereas the stock of DOC in Bilos groundwater was 0.08 kg m^{-2} during periods of high flow (Fig. 6). As a consequence, only a small

530 part of the soil organic C content was leached into groundwater during high flow periods. During these high flow periods, groundwater DOC peaked at a significantly higher value at the mesophylle to wet Landes station (Bilos), than at the mesophyll Landes (piezometer 3) and at the dry Landes (Piezometer 2) (Tab. 5). This is a consequence of the water table depth and amplitude and the content of C in the superficial layers of the soil (Fig. 4).

535 The three months (Mar. 2014-May. 2014) following the flood peak of 2014, DOC concentrations and stocks in Bilos groundwater decreased regularly in parallel with an increase in DIC concentrations and stocks in groundwater (Fig. 5b-c, 6). The DOC degradation and DIC accumulation rates in Bilos groundwater were very similar and estimated of about 60 mmol m^{-2} d^{-1}, or about 6.5 mmol m^{-3} d^{-1}, consistent with findings of Craft et al (2002) who reported respiration rates within the range of 3-100 mmol m^{-3} d^{-1} within a floodplain aquifer of a large gravel-bed river in north-western Montana in USA. In a

540 semi-arid mountain catchment in New Mexico, Baker et al (2000) also observed that groundwater DOC peaked during periods of high flow and resulted in higher rates of heterotrophic metabolism, presumably because of the supply of labile DOC via more intense hydrologic connections between the soil and groundwater. The bioavailability of groundwater DOC being related with the content of low molecular weight compounds, such as total dissolved amino acids (Shen et al., 2015); high molecular weight compounds, such as fulvic or humic acids are believed to be recalcitrant to decomposition by biota

545 (Baker et al., 2000). The second increase of DIC concentrations in groundwater during late summer of 2014 (Sep-Oct. 2014) was due to another process, this time not associated with any DOC degradation in groundwater (Fig. 5b-c). This DIC increase in late summer was concomitant with positive NEE and net heterotrophic conditions in the forest ecosystem (Fig. 2b, 5b). During drought period the soil water deficits stress the growing vegetation and leads to numerous physiological changes, including a decrease of the transpiration and the photosynthesis (Bray, 2001). The dehydration of plants lower the

550 rates of photosynthesis (i) directly by closing stomatal pores, hence interfering with uptake of carbon dioxide by leaves, and (ii) indirectly by adversely influencing the photosynthetic mechanism (Kozlowski, 2002). At our study site, the late summer period, when the forest ecosystem is a net source of CO_2 for the atmosphere, also corresponds to a maximum in CO_2 concentration in groundwater and thus a maximum contribution of soil respiration to groundwater DIC. To our best knowledge, this result is fully original. This warm period of the year is indeed favorable for a high production of gaseous

555 CO_2 in the unsaturated region of the soil (Lloyd and Taylor, 1994; Kätterer et al., 1998; Epron et al., 1999; Reth et al., 2009). In general, the transfer of CO_2 from soil air to groundwater after a long dry period occurs through percolation of rainwater in the unsaturated soil, as reported in an Amazonian plot (Johnson et al., 2008). However, at our study site, no rainy events occurred at that period (Fig. 2c), which suggests that soil CO_2 must have been transported to groundwater by another process such as simple downward diffusion (Fig. 7), that is also reported for transfer of O_2 between soil atmosphere and floodplain

560 aquifers (Malard and Hervant, 1999; Parker et al., 2014). Other authors noticed that during dry period a strong reduction in soil CO_2 flux to the atmosphere (upward diffusion) is associated with a decline in soil water content (Davidson et al., 1998;

Epron et al., 1999). In the Landes de Gascogne, during drought period, the high porosity in the sandy soil may favor downward diffusion of CO_2 and its dissolution in groundwater (Fig. 7). Thereafter, during early winter period, concentrations of DIC in groundwater decreased as a consequence of dilution with rainwater with low DIC content (Fig. 7).

4.3. Carbon transfer at the groundwater-stream-atmosphere interface

During the sampling period, groundwater exports DOC at a significantly higher value at the mesophyll to wet Landes station (Bilos, 0.9±0.9 mmol m^{-2} d^{-1}), than at the mesophyll Landes (Piezometer 3, 0.6±0.6 mmol m^{-2} d^{-1}) and at the dry Landes (Piezometer 2, 0.1±0.1 mmol m^{-2} d^{-1}) (Tab. 6). In contrast, groundwater exports DIC at the same order of magnitude at the wet and mesophyll Landes (0.9±0.5 mmol m^{-2} d^{-1} and 1.0±0.6 mmol m^{-2} d^{-1}, for Bilos and piezometer 3, respectively) that is significantly higher than at the dry Landes (0.6±0.4 mmol m^{-2} d^{-1}). In the Leyre watershed, C exports are influenced with the soil types, which are characterized with a different water table depth and amplitude (Fig. 4), as well as a gradient of C content in the different soil types. However, these last parameters have a stronger effect on the spatial heterogeneity of DOC exports than DIC exports (Tab. 6). Indeed, drainage and DOC concentrations in groundwater have a cumulative positive effect on DOC exports (Tab 2, 3, 5, 6; Fig. 5b-c); in contrast, drainage and DIC concentrations in groundwater have an antagonist effects on DIC exports (Tab 2, 3, 5, 6; Fig. 5b-c). As a consequence, groundwater exports the majority of DOC during high flow periods, but about the same quantity of DIC is exported during periods of high flow and periods of base flow (Tab. 6). In addition, during the study period the discharge varied by up to 100-fold (Fig. 2a); the corresponding variations in DIC and DOC concentrations and exports from the groundwater were up to 10 times (Tab. 5, 6; Fig. 4, 5). C export rates that are mainly determined by discharge and that the variations in C concentrations and exports are relatively small compared to the flow variation agree with other works (Fiedler et al., 2006; Öquist et al., 2009). However, for the whole sampling period, the mean weighted C export is almost the same both for DIC (0.9±0.5 mmol m^{-2} d^{-1}) and DOC (0.7±0.7 mmol m^{-2} d^{-1}) (Tab. 6), and, as drainage is the only hydrological pathway, the forest ecosystem exports in total 1.6±0.9 mmol m^{-2} d^{-1} (equivalents to 7.0±3.9 g C m^{-2} yr^{-1}), 40% as DOC and 60% as DIC (Tab. 6). This terrestrial C leaching from groundwater to streams is of the same order of magnitude of C leaching from subsoils (11.9±5.9 g C m^{-2} yr^{-1}) in five temperate forest plots across Europe (Kindler et al., 2011), or in a temperate Japan deciduous forests from soils to streams (4.0 g C m^{-2} yr^{-1}) (Shibata et al., 2005).

As in groundwater, DOC and DIC concentrations in first order streams were linearly negatively correlated (Tab. 3), suggesting that C dynamics in streams are mostly impacted by groundwater inputs (Kawasaki et al., 2005; Öquist et al., 2009). That is why, we observed higher DOC concentrations in streams during early winter and high flow periods than during growing season and late summer periods (Tab. 5) Increase in riverine DOC concentrations with discharge and high water table has been reported in the Leyre watershed (Polsenaere et al., 2013) and in many other forested catchments (Dawson et al., 2002; Striegl et al., 2005; Raymond and Saiers, 2010; Alvarez-Cobelas et al., 2012). At our study site, during periods of high flow, first order streams exported 0.2±0.2 mmol m^{-2} d^{-1} to second order streams; it is significantly lower than DOC exports (0.7±0.7 mmol m^{-2} d^{-1}) from groundwater to first order streams (Tab. 6). As a consequence, during the sampling period, 0.5 mmol m^{-2} d^{-1} of (equivalent to 2.2 g C m^{-2} yr^{-1}) of groundwater DOC is either degraded or re-adsorbed at

the groundwater-stream interface (Tab. 6). Indeed, when groundwater DOC enters the superficial river network through drainage part of it might be rapidly recycled by photo-oxidation (Macdonald and Minor, 2013; Moody and Worrall, 2016) and by respiration within the stream (Roberts et al., 2007; Hall Jr et al., 2016), or re-adsorbed on Fe-oxides at the river-bed oxic/anoxic interface. As a matter of fact, flocculation with Fe or Al can remove DOC from solution (Sharp et al., 2006). In contrast, DOC concentrations and exports in groundwater and streams were similar and stable during periods of base flow (Tab. 6). This suggests that groundwater DOC behaved conservatively during low flow stage (Schiff et al., 1997), and that DOC in streams was more labile during high flow stage (Aravena et al., 2004), increasing concentrations of labile DOC up to 27 fold in a small temperate and forested catchment in Pennsylvania USA (McLaughlin and Kaplan, 2013).

DIC concentration in streams increased in parallel with those in groundwater, during late summer period (Tab. 5; Fig. 5b). Indeed, concentrations of DIC show an inverse relationship with discharge in the Leyre watershed (Polsenaere et al., 2013) and in other temperate catchments (Billett et al., 2004; Dawson and Smith, 2007), as the result of dilution with rain water and lower contribution of deep CO_2-enriched groundwater during high flow periods The discharge of DIC-rich groundwater supersaturated with CO_2, together with the oxidation of dissolved organic matter in surface waters, results in a large CO_2 supersaturation of river (Stets et al., 2009). The quick loss of DIC concentrations between groundwater and first order streams is due to the degassing of CO_2 (Venkiteswaran et al., 2014). Efficient outgassing of CO_2 has been observed from headwaters with a large fraction of young groundwater (e.g., Fiedler et al., 2006). This rapid degassing was also attested by the change in the $\delta^{13}C$ signature of the DIC (Venkiteswaran et al., 2014; Deirmendjian and Abril, submitted). Furthermore, the positive correlation between degassing and export of DIC (Tab. 3) reveals that groundwater DIC is the main source of CO_2 degassing in superficial stream waters (Öquist et al.,2009) with low stream order (Hotchkiss et al., 2015). At our study site, this very fast degassing was confirmed by observations of Deirmendjian and Abril (submitted) where spring waters loosed 70% of their CO_2 in 40 meters downstream or with those of Öquist et al (2009) in boreal catchment who found that 65% of the DIC in the groundwater is lost within 200 meters of the water entering the stream. This also agree with with Venkiteswaran et al (2014) who concluded that most of the stream CO_2 originating in high CO_2 groundwater has been lost before typical in-stream sampling occurs. At our study site, throughout the sampling period degassing is on average 0.6±0.3 mmol m^{-2} d^{-1} (equivalent to 2.6±1.3 g C m^{-2} yr^{-1}). CO_2 degassing was higher during high flow periods than during periods of base flow (Tab. 6). This is a consequence of both higher inputs of groundwater DIC in streams during periods of high flow (Tab. 5) and higher water turbulence. As a matter of fact, degassing is a function of water velocity that induces water turbulence and thus increases the gas transfer velocity (Alin et al., 2011; Raymond et al., 2012). Finally, during the whole sampling period CO_2 degassing in streams represented about 65% of the DIC exported from groundwater and thus, a significant part of the carbon exported from forest plot rapidly returns in the atmosphere in the form of CO_2 through degassing.

Globally, if we consider the highest estimates of the different C fluxes (i.e., 2.1 Pg C yr^{-1} for degassing of CO_2, 0.23 Pg C yr^{-1} for organic C burial in sediments and 0.9 Pg C yr^{-1}, for C export to coastal systems; Meybeck, 1982; Cole et al., 2007; Raymond et al., 2013) occurring in inland waters (Cole et al., 2007), this would imply that the majority of the NEE (estimated to be 2.6±1.2 Pg C yr^{-1};Ciais et al., 2013), is being exported to the hydrological network. At our study site,

leaching of terrestrial C represents 1.6±0.9 mmol m^{-2} d^{-1} (equivalents to 7.0±3.9 g C m^{-2} yr^{-1}) whereas the net land sink is estimated at -90±110 mmol m^{-2} d^{-1} (equivalent to 390±480 g C m^{-2} yr^{-1}). As a consequence, leaching of terrestrial C represent a small (about 2%), but continuous loss of C from terrestrial ecosystems (Shibata et al., 2005; Kindler et al., 2011).

5. Conclusion

635 Monitoring DIC and DOC concentrations in groundwater and first order streams of the Leyre catchment brings new insights on the nature of processes that control C leaching from soils, transformation in groundwater and export to surface waters and back to the atmosphere (Fig. 7). This terrestrial-aquatic-atmosphere interface is believed to behave as a hotspot in the continental C cycle. The sandy acidic podzol soils have special feature that enable a clear temporal decomposition of processes in relation with hydrology, forest ecosystem production and respiration as monitored during the study. In winter, 640 the rise of the water table and the saturation of the topsoil, induce a large mobilization of soil organic matter as DOC to groundwater; DIC concentrations are minimum at this high water stage, although export (particularly of DOC) to surface waters is promoted by high drainage in winter. In spring and until summer, when groundwater disconnected from the topsoil, DOC concentrations and stocks decreased in association with an equivalent gain in DIC. This suggests that respiration in groundwater occurs at this season and acts as an important sink of DOC and a source of DIC. Later in dry summer 645 conditions, a second DIC peak occurred in groundwater, not associated with DOC consumption, but rather with high temperatures, low water table, and heterotrophic conditions in the forest ecosystem. These conditions probably result in high CO_2 concentrations in the air of the unsaturated soil and fast downward diffusion of CO_2 to deeper groundwater, favored by high porosity. Comparison of dissolved C concentrations between groundwater and streams reveal a fast degassing of DIC as CO_2 throughout the year. In contrast, groundwater DOC was exported conservatively to streams during base flow periods, 650 but not during winter high flow probably because of spatial heterogeneity in the landscape and fast degradation processes in streams or in the groundwater itself. Although spatial extrapolation of information from the plot scale to first order streams in the watershed generate some uncertainty, thanks to the relatively simple hydrological functioning of the watershed and our monitoring in three piezometers and six streams, we could make a comparison of stream C export with other fluxes in the landscape. Representing 2% of forest NEE, DIC and DOC exports are not very significant component of the C budget of 655 Landes de Gascogne ecosystems, dominated by *pinus pinaster* forest growing on podzol sandy soils.

Acknowledgments

This research is part of the CNP-Leyre project funded by the Cluster of Excellence COTE at the Université de Bordeaux (ANR-10-LABX-45). We thank Luiz Carlos Cotovicz Junior, Katixa Lajaunie-Salla, Baptiste Voltz, Gwenaëlle Chaillou and Damien Buquet (EPOC Bordeaux) for their assistance in the field. We thank Pierre Anshutz (EPOC, Bordeaux), Alain 660 Mollier and Christian Morel (ISPA INRA) for their implications on the CNP-Leyre project, and Céline Charbonnier for alkalinity titrations in the lab. Pierre Trichet (ISPA INRA) provided SOC data at the Bilos site.

Bibliography

Abril, G., Bouillon, S., Darchambeau, F., Teodoru, C.R., Marwick, T.R., Tamooh, F., Ochieng Omengo, F., Geeraert, N., Deirmendjian, L., Polsenaere, P., Borges, A.V., 2015. Technical Note: Large overestimation of pCO2 calculated from pH and alkalinity in acidic, organic-rich freshwaters. Biogeosciences 12, 67–78. doi:10.5194/bg-12-67-2015

Achat, D.L., Augusto, L., Morel, C., Bakker, M.R., 2011. Predicting available phosphate ions from physical–chemical soil properties in acidic sandy soils under pine forests. Journal of soils and sediments 11, 452–466.

Ahuja, L.R., Ma, L., Green, T.R., 2010. Effective soil properties of heterogeneous areas for modeling infiltration and redistribution. Soil Science Society of America Journal 74, 1469–1482.

Alin, S.R., de Fátima FL Rasera, M., Salimon, C.I., Richey, J.E., Holtgrieve, G.W., Krusche, A.V., Snidvongs, A., 2011. Physical controls on carbon dioxide transfer velocity and flux in low-gradient river systems and implications for regional carbon budgets. Journal of Geophysical Research: Biogeosciences 116.

Alley, W.M., Healy, R.W., LaBaugh, J.W., Reilly, T.E., 2002. Flow and storage in groundwater systems. science 296, 1985–1990.

Alvarez-Cobelas, M., Angeler, D.G., Sánchez-Carrillo, S., Almendros, G., 2012. A worldwide view of organic carbon export from catchments. Biogeochemistry 107, 275–293.

Aravena, R., Wassenaar, L.I., Spiker, E.C., 2004. Chemical and carbon isotopic composition of dissolved organic carbon in a regional confined methanogenic aquifer. Isotopes in environmental and health studies 40, 103–114.

Artinger, R., Buckau, G., Geyer, S., Fritz, P., Wolf, M., Kim, J.I., 2000. Characterization of groundwater humic substances: influence of sedimentary organic carbon. Applied Geochemistry 15, 97–116.

Atkins, M.L., Santos, I.R., Ruiz-Halpern, S., Maher, D.T., 2013. Carbon dioxide dynamics driven by groundwater discharge in a coastal floodplain creek. Journal of hydrology 493, 30–42.

Aubinet, M., Grelle, A., Ibrom, A., Rannik, Ü., Moncrieff, J., Foken, T., Kowalski, A.S., Martin, P.H., Berbigier, P., Bernhofer, C., vdv, 1999. Estimates of the annual net carbon and water exchange of forests: the EUROFLUX methodology. Advances in ecological research 30, 113–175.

Augusto, L., Badeau, V., Arrouays, D., Trichet, P., Flot, J.L., Jolivet, C., Merzeau, D., 2006. Caractérisation physico-chimique des sols à l'échelle d'une région naturelle à partir d'une compilation de données. Exemple des sols du massif forestier landais. Etude et gestion des sols 13, 7–22.

Augusto, L., Bakker, M.R., Morel, C., Meredieu, C., Trichet, P., Badeau, V., Arrouays, D., Plassard, C., Achat, D.L., Gallet-Budynek, A., Merzeau, D., Canteloup, D., Najar, M., Ranger, J., 2010. Is "grey literature" a reliable source of data to characterize soils at the scale of a region? A case study in a maritime pine forest in southwestern France. European Journal of Soil Science 61, 807–822. doi:10.1111/j.1365-2389.2010.01286.x

Baker, M.A., Valett, H.M., Dahm, C.N., 2000. Organic carbon supply and metabolism in a shallow groundwater ecosystem. Ecology 81, 3133–3148.

Bakker, M.R., Augusto, L., Achat, D.L., 2006. Fine root distribution of trees and understory in mature stands of maritime pine (Pinus pinaster) on dry and humid sites. Plant and Soil 286, 37–51.

Bakker, M.R., Jolicoeur, E., Trichet, P., Augusto, L., Plassard, C., Guinberteau, J., Loustau, D., 2009. Adaptation of fine roots to annual fertilization and irrigation in a 13-year-old Pinus pinaster stand. Tree physiology 29, 229–238.

Bertran, P., Allenet, G., Gé, T., Naughton, F., Poirier, P., Goñi, M.F.S., 2009. Coversand and Pleistocene palaeosols in the Landes region, southwestern France. Journal of Quaternary Science 24, 259–269.

Bertran, P., Bateman, M.D., Hernandez, M., Mercier, N., Millet, D., Sitzia, L., Tastet, J.-P., 2011. Inland aeolian deposits of south-west France: facies, stratigraphy and chronology. Journal of Quaternary Science 26, 374–388.

Billett, M.F., Palmer, S.M., Hope, D., Deacon, C., Storeton-West, R., Hargreaves, K.J., Flechard, C., Fowler, D., 2004. Linking land-atmosphere-stream carbon fluxes in a lowland peatland system. Global Biogeochemical Cycles 18.

Bolan, N.S., Adriano, D.C., Kunhikrishnan, A., James, T., McDowell, R., Senesi, N., 2011. Dissolved organic matter: biogeochemistry, dynamics, and environmental significance in soils. Advances in agronomy 110, 1.

Bosch, J.M., Hewlett, J.D., 1982. A review of catchment experiments to determine the effect of vegetation changes on water yield and evapotranspiration. Journal of hydrology 55, 3–23.

Bray, E.A., 2001. Plant Response to Water-deficit Stress, in: John Wiley & Sons, Ltd (Ed.), Encyclopedia of Life Sciences. John Wiley & Sons, Ltd, Chichester. doi:10.1038/npg.els.0001298

Butman, D., Raymond, P.A., 2011. Significant efflux of carbon dioxide from streams and rivers in the United States. Nature Geosci 4, 839–842. doi:10.1038/ngeo1294

Camino-Serrano, M., Gielen, B., Luyssaert, S., Ciais, P., Vicca, S., Guenet, B., Vos, B.D., Cools, N., Ahrens, B., Altaf Arain, M., others, 2014. Linking variability in soil solution dissolved organic carbon to climate, soil type, and vegetation type. Global Biogeochemical Cycles 28, 497–509.

Ciais, P., Sabine, C., Bala, G., Bopp, L., Brovkin, V., Canadell, J., Chhabra, A., DeFries, R., Galloway, J., Heimann, M., Jones, C., Le Quéré, C., Myeni, R.., Piao, S., Thornton, P., 2013. Carbon and other biogeochemical cycles, in: Climate Change 2013: The Physical Science Basis. Contribution of Working Group I to the Fifth Assessment Report of the Intergovernmental Panel on Climate Change. Cambridge University Press, Cambridge, United Kingdom and New York, NY, USA., pp. 465–570.

Cole, J.J., Prairie, Y.T., Caraco, N.F., McDowell, W.H., Tranvik, L.J., Striegl, R.G., Duarte, C.M., Kortelainen, P., Downing, J.A., Middelburg, J.J., Melack, J., 2007. Plumbing the Global Carbon Cycle: Integrating Inland Waters into the Terrestrial Carbon Budget. Ecosystems 10, 171–184. doi:10.1007/s10021-006-9013-8

Corbier, P., Karnay, G., Bourgine, B., Saltel, M., 2010. Gestion des eaux souterraines en région Aquitaine. Reconnaissance des potentialités aquiferes du Mio-Plio-Quaternaire des Landes de Gascogne et du Médoc en relation avec les SAGE. No. Rapport final, BRGM RP 57813.

Craft, J.A., Stanford, J.A., Pusch, M., 2002. Microbial respiration within a floodplain aquifer of a large gravel-bed river. Freshwater Biology 47, 251–261.

Datry, T., Malard, F., Gibert, J., 2004. Dynamics of solutes and dissolved oxygen in shallow urban groundwater below a stormwater infiltration basin. Science of the Total Environment 329, 215–229.

David, T.S., Pinto, C.A., Nadezhdina, N., Kurz-Besson, C., Henriques, M.O., Quilhó, T., Cermak, J., Chaves, M.M., Pereira, J.S., David, J.S., 2013. Root functioning, tree water use and hydraulic redistribution in Quercus suber trees: a modeling approach based on root sap flow. Forest Ecology and Management 307, 136–146.

Davidson, E., Belk, E., Boone, R.D., others, 1998. Soil water content and temperature as independent or confounded factors controlling soil respiration in a temperate mixed hardwood forest. Global change biology 4, 217–227.

Dawson, J.J., Smith, P., 2007. Carbon losses from soil and its consequences for land-use management. Science of the total environment 382, 165–190.

Dawson, J.J.C., Billett, M.F., Neal, C., Hill, S., 2002. A comparison of particulate, dissolved and gaseous carbon in two contrasting upland streams in the UK. Journal of Hydrology 257, 226–246.

Delprat, L., 1997. Caractérisation du carbone organique soluble sous monoculture de maïs en sol sableux landais. Influence sur les émissions de protoxyde d'azote.

Deirmendjian, L., Abril, G., submitted. Carbon dioxide degassing at the groundwater-stream-atmosphere interface: isotopic equilibration and hydrological mass balance in a sandy watershed. Journal of hydrology.

Dinsmore, K.J., Billett, M.F., Skiba, U.M., Rees, R.M., Drewer, J., Helfter, C., 2010. Role of the aquatic pathway in the carbon and greenhouse gas budgets of a peatland catchment. Global Change Biology 16, 2750–2762.

Einarsdottir, K., Wallin, M.B., Sobek, S., 2017. High terrestrial carbon load via groundwater to a boreal lake dominated by surface water inflow. Journal of Geophysical Research: Biogeosciences 122, 15–29.

Epron, D., Farque, L. etitia, Lucot, É., Badot, P.-M., 1999. Soil CO2 efflux in a beech forest: dependence on soil temperature and soil water content. Annals of Forest Science 56, 221–226.

Evans, C.D., Monteith, D.T., Cooper, D.M., 2005. Long-term increases in surface water dissolved organic carbon: observations, possible causes and environmental impacts. Environmental Pollution 137, 55–71.

Fang, W., Wei, Y., Liu, J., Kosson, D.S., van der Sloot, H.A., Zhang, P., 2016. Effects of aerobic and anaerobic biological processes on leaching of heavy metals from soil amended with sewage sludge compost. Waste Management 58, 324–334.

Ferro-Vázquez, C., Nóvoa-Muñoz, J.C., Costa-Casais, M., Klaminder, J., Martínez-Cortizas, A., 2014. Metal and organic matter immobilization in temperate podzols: A high resolution study. Geoderma 217–218, 225–234. doi:10.1016/j.geoderma.2013.10.006

Fiedler, S., Höll, B.S., Jungkunst, H.F., 2006. Discovering the importance of lateral CO 2 transport from a temperate spruce forest. Science of the total environment 368, 909–915.

760 Foken, T., Wichura, B., 1996. Tools for quality assessment of surface-based flux measurements. Agricultural and forest meteorology 78, 83–105.

Frankignoulle, M., Borges, A.V., 2001. Direct and Indirect pCO2 Measurements in a Wide Range of pCO2 and Salinity Values (The Scheldt Estuary). Aquatic Geochemistry 7, 267–273. doi:10.1023/A:1015251010481

Goldscheider, N., Hunkeler, D., Rossi, P., 2006. Microbial biocenoses in pristine aquifers and an assessment of investigative
765 methods. Hydrogeology Journal 14, 926–941.

Govind, A., Bonnefond, J.-M., Kumari, J., Moisy, C., Loustau, D., Wigneron, J.-P., 2012. Modeling the ecohydrological processes in the Landes de Gascogne, SW France, in: Plant Growth Modeling, Simulation, Visualization and Applications (PMA), 2012 IEEE Fourth International Symposium on. IEEE, pp. 133–140.

Guillot, M., Dayau, S., Spannraft, K., Guyon, D., Wigneron, J.-P., Loustau, D., 2010. Study of two forested watersheds in
770 Les Landes region: monitoring of carbon stock and water cycle over the last decades.

Hagedorn, F., Kaiser, K., Feyen, H., Schleppi, P., 2000. Effects of redox conditions and flow processes on the mobility of dissolved organic carbon and nitrogen in a forest soil. Journal of Environmental Quality 29, 288–297.

Hall Jr, R.O., Tank, J.L., Baker, M.A., Rosi-Marshall, E.J., Hotchkiss, E.R., 2016. Metabolism, gas exchange, and carbon spiraling in rivers. Ecosystems 19, 73–86.

775 Heimann, M., Reichstein, M., 2008. Terrestrial ecosystem carbon dynamics and climate feedbacks. Nature 451, 289–292.

Hotchkiss, E.R., Hall Jr, R.O., Sponseller, R.A., Butman, D., Klaminder, J., Laudon, H., Rosvall, M., Karlsson, J., 2015. Sources of and processes controlling CO2 emissions change with the size of streams and rivers. Nature Geoscience 8, 696–699.

Ibrom, A., Dellwik, E., Flyvbjerg, H., Jensen, N.O., Pilegaard, K., 2007. Strong low-pass filtering effects on water vapour
780 flux measurements with closed-path eddy correlation systems. Agricultural and Forest Meteorology 147, 140–156.

Inamdar, S., Finger, N., Singh, S., Mitchell, M., Levia, D., Bais, H., Scott, D., McHale, P., 2012. Dissolved organic matter (DOM) concentration and quality in a forested mid-Atlantic watershed, USA. Biogeochemistry 108, 55–76.

Johnson, M.S., Lehmann, J., Couto, E.G., Novaes Filho, J.P., Riha, S.J., 2006. DOC and DIC in flowpaths of Amazonian headwater catchments with hydrologically contrasting soils. Biogeochemistry 81, 45–57.

785 Johnson, M.S., Lehmann, J., Riha, S.J., Krusche, A.V., Richey, J.E., Ometto, J.P.H., Couto, E.G., 2008. CO2 efflux from Amazonian headwater streams represents a significant fate for deep soil respiration. Geophysical Research Letters 35.

Jolivet, C., Augusto, L., Trichet, P., Arrouays, D., 2007. Forest soils in the Gascony Landes Region: formation, history, properties and spatial varaibility [WWW Document]. URL http://hdl.handle.net/2042/8480

790 Jonsson, A., Algesten, G., Bergström, A.-K., Bishop, K., Sobek, S., Tranvik, L.J., Jansson, M., 2007. Integrating aquatic carbon fluxes in a boreal catchment carbon budget. Journal of Hydrology 334, 141–150.

Kaimal, J.C., Finnigan, J.J., 1994. Atmospheric boundary layer flows: their structure and measurement. Oxford University Press.

Kaiser, K., Guggenberger, G., 2000. The role of DOM sorption to mineral surfaces in the preservation of organic matter in
795 soils. Organic geochemistry 31, 711–725.

Kaiser, K., Guggenberger, G., Zech, W., 1996. Sorption of DOM and DOM fractions to forest soils. Geoderma 74, 281–303.

Kalbitz, K., Kaiser, K., 2008. Contribution of dissolved organic matter to carbon storage in forest mineral soils. Journal of Plant Nutrition and Soil Science 171, 52–60.

Kalbitz, K., Solinger, S., Park, J.-H., Michalzik, B., Matzner, E., 2000. Controls on the dynamics of dissolved organic matter
800 in soils: a review. Soil science 165, 277–304.

Kätterer, T., Reichstein, M., Andrén, O., Lomander, A., 1998. Temperature dependence of organic matter decomposition: a critical review using literature data analyzed with different models. Biology and fertility of soils 27, 258–262.

Kawasaki, M., Ohte, N., Katsuyama, M., 2005. Biogeochemical and hydrological controls on carbon export from a forested catchment in central Japan. Ecological Research 20, 347–358.

805 Kindler, R., Siemens, J.A.N., Kaiser, K., Walmsley, D.C., Bernhofer, C., Buchmann, N., Cellier, P., Eugster, W., Gleixner, G., GRÜNWALD, T., others, 2011. Dissolved carbon leaching from soil is a crucial component of the net ecosystem carbon balance. Global Change Biology 17, 1167–1185.

Kokic, J., Wallin, M.B., Chmiel, H.E., Denfeld, B.A., Sobek, S., 2015. Carbon dioxide evasion from headwater systems strongly contributes to the total export of carbon from a small boreal lake catchment. Journal of Geophysical Research: Biogeosciences 120, 2014JG002706. doi:10.1002/2014JG002706

Kowalski, S., Sartore, M., Burlett, R., Berbigier, P., Loustau, D., 2003. The annual carbon budget of a French pine forest (Pinus pinaster) following harvest. Global Change Biology 9, 1051–1065.

Kozlowski, T.T., 2002. Physiological-ecological impacts of flooding on riparian forest ecosystems. Wetlands 22, 550–561.

Legigan, P., 1979. L'élaboration de la formation du sable des Landes, dépôt résiduel de l'environnement sédimentaire pliocène-pléïstocène centre aquitain. Institut de géologie du Bassin d'Aquitaine.

Leith, F.I., Dinsmore, K.J., Wallin, M.B., Billett, M.F., Heal, K.V., Laudon, H., Öquist, M.G., Bishop, K., 2015. Carbon dioxide transport across the hillslope–riparian–stream continuum in a boreal headwater catchment. Biogeosciences 12, 1881–1892. doi:10.5194/bg-12-1881-2015

Lewis, E., Wallace, D., Allison, L.J., 1998. Program developed for CO2 system calculations. Carbon Dioxide Information Analysis Center, managed by Lockheed Martin Energy Research Corporation for the US Department of Energy Tennessee.

Lloyd, J., Taylor, J.A., 1994. On the temperature dependence of soil respiration. Functional ecology 315–323.

Loustau, D., Granier, A., El Hadj Moussa, F., 1990. Seasonal variations of sap flow in a maritime pine standard [hydraulic conductance, stomatal conductance]. Annales des Sciences Forestieres (France).

Loustau, D., Guillot, M., 2009. Impact écologique de la tempête et conséquences sur les cycles de l'eau et du carbone.

Lundström, U.S., van Breemen, N., Bain, D., 2000. The podzolization process. A review. Geoderma 94, 91–107.

Lundström, U. van, Van Breemen, N., Bain, D.C., Van Hees, P.A.W., Giesler, R., Gustafsson, J.P., Ilvesniemi, H., Karltun, E., Melkerud, P.-A., Olsson, M., others, 2000. Advances in understanding the podzolization process resulting from a multidisciplinary study of three coniferous forest soils in the Nordic Countries. Geoderma 94, 335–353.

Luyssaert, S., Ciais, P., Piao, S.L., SCHULZE, E.-D., Jung, M., Zaehle, S., Schelhaas, M.J., Reichstein, M., Churkina, G., Papale, D., others, 2010. The European carbon balance. Part 3: forests. Global Change Biology 16, 1429–1450.

Macdonald, M.J., Minor, E.C., 2013. Photochemical degradation of dissolved organic matter from streams in the western Lake Superior watershed. Aquatic sciences 75, 509–522.

Malard, F., Hervant, F., 1999. Oxygen supply and the adaptations of animals in groundwater. Freshwater Biology 41, 1–30.

McClain, M.E., Boyer, E.W., Dent, C.L., Gergel, S.E., Grimm, N.B., Groffman, P.M., Hart, S.C., Harvey, J.W., Johnston, C.A., Mayorga, E., others, 2003. Biogeochemical hot spots and hot moments at the interface of terrestrial and aquatic ecosystems. Ecosystems 6, 301–312.

McLaughlin, C., Kaplan, L.A., 2013. Biological lability of dissolved organic carbon in stream water and contributing terrestrial sources. Freshwater Science 32, 1219–1230.

Mendes, M.P., Ribeiro, L., David, T.S., Costa, A., 2016. How dependent are cork oak (Quercus suber L.) woodlands on groundwater? A case study in southwestern Portugal. Forest Ecology and Management 378, 122–130.

Meybeck, M., 1982. Carbon, nitrogen, and phosphorus transport by world rivers. Am. J. Sci 282, 401–450.

Michalzik, B., Kalbitz, K., Park, J.-H., Solinger, S., Matzner, E., 2001. Fluxes and concentrations of dissolved organic carbon and nitrogen–a synthesis for temperate forests. Biogeochemistry 52, 173–205.

Millero, F.J., 1979. The thermodynamics of the carbonate system in seawater. Geochimica et Cosmochimica Acta 43, 1651–1661.

Moody, C.S., Worrall, F., 2016. Sub-daily rates of degradation of fluvial carbon from a peat headwater stream. Aquatic Sciences 78, 419–431.

Moreaux, V., Lamaud, É., Bosc, A., Bonnefond, J.-M., Medlyn, B.E., Loustau, D., 2011. Paired comparison of water, energy and carbon exchanges over two young maritime pine stands (Pinus pinaster Ait.): effects of thinning and weeding in the early stage of tree growth. Tree physiology tpr048.

Naumburg, E., Mata-Gonzalez, R., Hunter, R.G., Mclendon, T., Martin, D.W., 2005. Phreatophytic vegetation and groundwater fluctuations: a review of current research and application of ecosystem response modeling with an emphasis on Great Basin vegetation. Environmental Management 35, 726–740.

Oki, T., Kanae, S., 2006. Global hydrological cycles and world water resources. science 313, 1068–1072.

Olefeldt, D., Roulet, N., Giesler, R., Persson, A., 2013. Total waterborne carbon export and DOC composition from ten nested subarctic peatland catchments—importance of peatland cover, groundwater influence, and inter-annual variability of precipitation patterns. Hydrological Processes 27, 2280–2294.

Öquist, M.G., Wallin, M., Seibert, J., Bishop, K., Laudon, H., 2009. Dissolved inorganic carbon export across the soil/stream interface and its fate in a boreal headwater stream. Environmental science & technology 43, 7364–7369.

Pabich, W.J., Valiela, I., Hemond, H.F., 2001. Relationship between DOC concentration and vadose zone thickness and depth below water table in groundwater of Cape Cod, USA. Biogeochemistry 55, 247–268.

Parker, S.R., Darvis, M.N., Poulson, S.R., Gammons, C.H., Stanford, J.A., 2014. Dissolved oxygen and dissolved inorganic carbon stable isotope composition and concentration fluxes across several shallow floodplain aquifers and in a diffusion experiment. Biogeochemistry 117, 539–552.

Polsenaere, P., Abril, G., 2012. Modelling CO_2 degassing from small acidic rivers using water pCO_2, DIC and $\delta^{13}C$-DIC data. Geochimica et Cosmochimica Acta 91, 220–239. doi:10.1016/j.gca.2012.05.030

Polsenaere, P., Savoye, N., Etcheber, H., Canton, M., Poirier, D., Bouillon, S., Abril, G., 2013a. Export and degassing of terrestrial carbon through watercourses draining a temperate podzolized catchment. Aquatic sciences 75, 299–319.

Raymond, P.A., Hartmann, J., Lauerwald, R., Sobek, S., McDonald, C., Hoover, M., Butman, D., Striegl, R., Mayorga, E., Humborg, C., Kortelainen, P., Dürr, H., Meybeck, M., Ciais, P., Guth, P., 2013. Global carbon dioxide emissions from inland waters. Nature 503, 355–359. doi:10.1038/nature12760

Raymond, P.A., Saiers, J.E., 2010. Event controlled DOC export from forested watersheds. Biogeochemistry 100, 197–209.

Raymond, P.A., Zappa, C.J., Butman, D., Bott, T.L., Potter, J., Mulholland, P., Laursen, A.E., McDowell, W.H., Newbold, D., 2012. Scaling the gas transfer velocity and hydraulic geometry in streams and small rivers. Limnology and Oceanography: Fluids and Environments 2, 41–53.

Regnier, P., Friedlingstein, P., Ciais, P., Mackenzie, F.T., Gruber, N., Janssens, I.A., Laruelle, G.G., Lauerwald, R., Luyssaert, S., Andersson, A.J., Arndt, S., Arnosti, C., Borges, A.., Dale, A.., Gallego-Sala, A., Goddéris, Y., Goosens, N., Hartmann, J., Heinze, C., Ilyina, T., Joos, F., LaRowe, D.., Leifeld, J., Meysman, J.., Munhoven, G., Raymond, P.., Spahni, R., Suntharalingam, P., Thullner, M., 2013. Anthropogenic perturbation of the carbon fluxes from land to ocean. Nature Geoscience 6, 597–607.

Reichstein, M., Falge, E., Baldocchi, D., Papale, D., Aubinet, M., Berbigier, P., Bernhofer, C., Buchmann, N., Gilmanov, T., Granier, A., others, 2005. On the separation of net ecosystem exchange into assimilation and ecosystem respiration: review and improved algorithm. Global Change Biology 11, 1424–1439.

Reth, S., Graf, W., Reichstein, M., Munch, J.C., 2009. Sustained stimulation of soil respiration after 10 years of experimental warming. Environmental Research Letters 4, 024005.

Roberts, B.J., Mulholland, P.J., Hill, W.R., 2007. Multiple scales of temporal variability in ecosystem metabolism rates: results from 2 years of continuous monitoring in a forested headwater stream. Ecosystems 10, 588–606.

Sadat-Noori, M., Maher, D.T., Santos, I.R., 2016. Groundwater discharge as a source of dissolved carbon and greenhouse gases in a subtropical estuary. Estuaries and Coasts 39, 639–656.

Sanderman, J., Amundson, R., 2009. A comparative study of dissolved organic carbon transport and stabilization in California forest and grassland soils. Biogeochemistry 92, 41–59.

Santos, I.R., Maher, D.T., Eyre, B.D., 2012. Coupling automated radon and carbon dioxide measurements in coastal waters. Environmental science & technology 46, 7685–7691.

Sauer, D., Sponagel, H., Sommer, M., Giani, L., Jahn, R., Stahr, K., 2007. Podzol: Soil of the year 2007. A review on its genesis, occurrence, and functions. Journal of Plant Nutrition and Soil Science 170, 581–597.

Schiff, S.L., Aravena, R., Trumbore, S.E., Hinton, M.J., Elgood, R., Dillon, P.J., 1997. Export of DOC from forested catchments on the Precambrian Shield of Central Ontario: clues from 13C and 14C. Biogeochemistry 36, 43–65.

Sharp, E.L., Jarvis, P., Parsons, S.A., Jefferson, B., 2006. Impact of fractional character on the coagulation of NOM. Colloids and Surfaces A: Physicochemical and Engineering Aspects 286, 104–111.

Sharp, J.H., 1993. The dissolved organic carbon controversy: an update. Oceanography 6.

Shen, Y., Chapelle, F.H., Strom, E.W., Benner, R., 2015. Origins and bioavailability of dissolved organic matter in groundwater. Biogeochemistry 122, 61–78.

Shibata, H., Hiura, T., Tanaka, Y., Takagi, K., Koike, T., 2005. Carbon cycling and budget in a forested basin of southwestern Hokkaido, northern Japan. Ecological Research 20, 325–331.

Shibata, H., Mitsuhashi, H., Miyake, Y., Nakano, S., 2001. Dissolved and particulate carbon dynamics in a cool-temperate forested basin in northern Japan. Hydrological Processes 15, 1817–1828.

Stets, E.G., Striegl, R.G., Aiken, G.R., Rosenberry, D.O., Winter, T.C., 2009. Hydrologic support of carbon dioxide flux revealed by whole-lake carbon budgets. Journal of geophysical research: Biogeosciences 114.

910 Striegl, R.G., Aiken, G.R., Dornblaser, M.M., Raymond, P.A., Wickland, K.P., 2005. A decrease in discharge-normalized DOC export by the Yukon River during summer through autumn. Geophysical Research Letters 32.

Sun, G., Riekerk, H., Kornhak, L.V., 2000. Ground-water-table rise after forest harvesting on cypress-pine flatwoods in Florida. Wetlands 20, 101–112.

Thivolle-Cazat, A., Najar, M., 2001. Évolution de la productivité et de la récolte du pin maritime dans le massif Landais.
915 Evaluation de la disponibilité future en Gironde. Revue forestière française 53, 351–355.

Thornthwaite, C.W., 1948. An approach toward a rational classification of climate. Geographical review 38, 55–94.

Venkiteswaran, J.J., Schiff, S.L., Wallin, M.B., 2014. Large Carbon Dioxide Fluxes from Headwater Boreal and Sub-Boreal Streams. PLoS ONE 9, e101756. doi:10.1371/journal.pone.0101756

Vernier, F., Castro, A., 2010. Critère Préservation de l'environnement Sous-critère Eau.

920 Vincke, C., Thiry, Y., 2008. Water table is a relevant source for water uptake by a Scots pine (Pinus sylvestris L.) stand: Evidences from continuous evapotranspiration and water table monitoring. Agricultural and Forest Meteorology 148, 1419–1432.

Vissers, M.J., van der Perk, M., 2008. The stability of groundwater flow systems in unconfined sandy aquifers in the Netherlands. Journal of hydrology 348, 292–304.

925 Wallin, M.B., Grabs, T., Buffam, I., Laudon, H., Ågren, A., Öquist, M.G., Bishop, K., 2013. Evasion of CO2 from streams – The dominant component of the carbon export through the aquatic conduit in a boreal landscape. Glob Change Biol 19, 785–797. doi:10.1111/gcb.12083

Weiss, R., 1974. Carbon dioxide in water and seawater: the solubility of a non-ideal gas. Marine chemistry 2, 203–215.

Wilson, H.F., Saiers, J.E., Raymond, P.A., Sobczak, W.V., 2013. Hydrologic drivers and seasonality of dissolved organic
930 carbon concentration, nitrogen content, bioavailability, and export in a forested New England stream. Ecosystems 16, 604–616.

Xu, Y.-J., Burger, J.A., Aust, W.M., Patterson, S.C., Miwa, M., Preston, D.P., 2002. Changes in surface water table depth and soil physical properties after harvest and establishment of loblolly pine (Pinus taeda L.) in Atlantic coastal plain wetlands of South Carolina. Soil and Tillage Research 63, 109–121.

935

	Abbreviations	Definitions
Hydrological parameters	P	Precipitation at the Bilos site (mm d^{-1})
	GWS	Groundwater storage at the Bilos site (mm d^{-1})
	ETR	Evapotranspiration at the Bilos site (mm d^{-1})
	D	Drainage of shallow groundwater by first order streams (mm d^{-1})
	H	Groundwater table depth at the Bilos site (mm)
	H$_m$	Mean groundwater table depth at the Bilos site (mm)
Hydrological periods	HF	High flow period (Jan. 2014-Mar. 2014 and Feb. 2015-Mar. 2015)
	GS	Growing season period (Apr. 2014-Aug. 2014 and Apr. 2015-Aug. 2015)
	LS	Late summer period (Sep. 2014-Oct. 2014 and Sep. 2015-Oct. 2015)
	EW	Early winter period (Nov. 2014-Jan. 2015 and Nov. 2015-Dec. 2015)
	BF	Base flow period (GS+LS+EW)
Carbon parameters	C	Carbon
	TA	Total Alkalinity (µmol L^{-1})
	pCO$_2$	Partial pressure of CO$_2$ (ppmv)
	DIC	Dissolved inorganic carbon
	DOC	Dissolved organic carbon
	DIC$_m$	Mean concentration of DIC in Bilos groundwater (mmol m^{-3})
	DOC$_m$	Mean concentration of DOC in Bilos groundwater (mmo m^{-3})
	DIC$_{m1}$	Mean concentration of DIC in first order streams (mmol m^{-3})
	DOC$_{m1}$	Mean concentration of DOC in first order streams (mmol m^{-3})
Carbon stocks and fluxes	DIC$_{stock}$	Stock of DIC in groundwater (mmol m^{-2})
	DOC$_{stock}$	Stock of DOC in groundwater (mmol m^{-2})
	DIC$_{export}$	Export of DIC through drainage of shallow groundwater (mmol m^{-2} d^{-1})
	DOC$_{export}$	Export of DOC through drainage of shallow groundwater (mmol m^{-2} d^{-1})
	F$_{degass}$	Degassing in first order streams (mmol m^{-2} d^{-1})
	GPP	Gross Primary Production at the Bilos site (mmol m^{-2} d^{-1})
	R$_{eco}$	Respiration of the ecosystem at the Bilos site (mmol m^{-2} d^{-1})
	NEE	Net Ecosystem Exchange, calculated as R$_{eco}$ – GPP at the Bilos site (mmol m^{-2} d^{-1})

Table 1: Abbreviations used in the paper.

	Precipitation (P)	Evapotranspiration (ETR)	Drainage (D)	Groundwater storage (GWS)
2014	1,102	912	191	-72
2015	691	621	108	-174
HF	4.7±2.1	2.4±1.0	1.1±0.4	-0.2
	[2.2~8.0]	[0.9~3.6]	[0.7~1.9]	[-2.9~4.0]
GS	1.8±0.8	3.0±0.9	0.3±0.2	-1.9
	[0.8~2.9]	[1.6~5.3]	[0.1~0.7]	[-3.1~-0.5]
LS	1.1±0.5	1.5±0.5	0.1±0.007	0.1
	[0.2~1.5]	[1.0~2.2]	[0.1~0.1]	[-1.2~0.7]
EW	2.7±1.5	0.5±0.2	0.2±0.07	1.9
	[0.2~4.7]	[0.3~0.7]	[0.1~0.3]	[0.7~4.5]

Table 2: Water budget of the Bilos plot scale for the year 2014 and 2015, as well as for high flow (HF), growing season (GS), late summer (LS) and early winter (EW) periods. For, HF, GS, LS and EW, numbers represent the mean±SD and the range (between square brackets) of each hydrological period. P, ETR, D and GWS are in mm for the year 2014 and 2015, and in mm d^{-1} for the other hydrological periods.

	DIC_m	DOC_m	DIC_{m1}	DOC_{m1}	DIC_{stock}	DOC_{stock}	DIC_{export}	DOC_{export}	F_{degass}	P	GWS	ETR	D	H_m	NEE	GPP	R
DIC_m	1	**-0.65**	**_0.86_**	-0.34	**_0.99_**	**-0.65**	-0.44	**-0.62**	-0.48	-0.02	0.45	-0.41	**-0.68**	**_-0.83_**	**0.52**	-0.31	-0.09
DOC_m		1	-0.41	0.43	**-0.64**	**_0.98_**	**0.69**	**_0.95_**	**0.56**	0.17	-0.28	0.41	**_0.93_**	**_0.85_**	-0.19	-0.13	-0.36
DIC_{m1}			1	**-0.55**	**_0.82_**	-0.42	-0.35	-0.34	**-0.54**	-0.14	0.23	-0.25	-0.44	**-0.75**	0.43	-0.32	-0.16
DOC_{m1}				1	-0.33	0.45	0.45	0.38	**0.66**	0.30	0.35	-0.39	0.46	**-0.70**	0.15	-0.41	**-0.53**
DIC_{stock}					1	**-0.63**	0.37	**-0.62**	-0.44	-0.04	0.45	-0.44	**0.67**	**-0.79**	-0.48	0.28	-0.07
DOC_{stock}						1	**_-0.82_**	**_0.97_**	**0.67**	0.21	-0.23	0.32	**_-0.97_**	**_0.88_**	0.20	-0.14	-0.39
DIC_{export}							1	**0.72**	**_0.86_**	0.26	0.01	0.02	**_0.83_**	**0.76**	-0.18	-0.15	-0.39
DOC_{export}								1	**0.57**	0.24	-0.22	0.28	**_0.98_**	**_0.81_**	-0.19	-0.17	-0.41
F_{degass}									1	0.45	0.24	0.17	**0.70**	**_0.78_**	0.06	-0.35	**-0.50**
P										1	**0.76**	-0.30	0.29	0.23	0.33	-0.44	-0.43
GWS											1	**-0.73**	-0.16	-0.15	**0.62**	**-0.63**	**-0.51**
ETR												1	0.22	0.17	**-0.63**	**0.63**	**0.50**
D													1	**_0.88_**	-0.23	-0.15	-0.41
H_m														1	-0.27	-0.06	0.31
NEE															1	**_-0.85_**	**-0.55**
GPP																1	**_0.91_**
R																	1

Table 3: Linear correlation (Pearson) between the studied parameters at the Bilos plot scale, during the sampling period. Numbers represent the Pearson's correlation coefficient at the Bilos plot between mean C concentrations in Bilos groundwater (DIC_m, DOC_m) and in the 6 first order streams (DIC_{m1}, DOC_{m1}), C exports (DIC_{export} and DOC_{export}), C stocks (DIC_{stock} and DOC_{stock}), hydrological parameters (P, GWS, ETR, D and H_m), metabolic parameters (NEE, GPP, R_{eco}) and degassing in the 6 first order streams (F_{degass}). Here, F_{degass} was calculated from the DIC data of the Bilos groundwater only. Each parameter was integrated between two sampling dates. Values in bold indicate correlation with p-value < 0.05, whereas underlined and bolded values indicate correlation with p-value < 0.001.

	GPP	R_{eco}	NEE
	mmol m^{-2} d^{-1}	mmol m^{-2} d^{-1}	mmol m^{-2} d^{-1}
2014-2015	400±210	310±150	-90±110
	[160~880]	[110~660]	[-340~100]
HF	300±80	180±50	-120±50
	[180~420]	[105~260]	[-160~-30]
GS	640±150	490±100	-160±140
	[380~880]	[320~640]	[-330~100]
LS	350±120	300±80	-50±60
	[240~540]	[200~410]	[-160~10]
EW	210±30	230±50	20±20
	[160~260]	[170~320]	[-10~65]

Table 4: Metabolic parameters (GPP, R_{eco} and NEE) estimated at the Bilos plot with the Eddy covariance techniques. Numbers represent the mean±SD and the
950 range (between square brackets) for the 2014-2015 period, and for high flow (HF), growing season (GS), late summer (LS) and early winter (EW) periods

Period	DIC (µmol L^{-1})				DOC (µmol L^{-1})			
	Piezometer Bilos	Piezometer 2	Piezometer 3	Streams	Piezometer Bilos	Piezometer 2	Piezometer 3	Streams
HF	1,160±470 [570~1,700]	1,380	1,510	280±40 [220~310]	3,500±200 [3,200~3,700]	280	1,500	490±10 [460~510]
GS	2,570±240 [2,350~3,030]	1,450±380 [1,000~2,100]	2,030±220 [1,650~2,160]	330±120 [210~550]	750±440 [320~950]	380±40 [300~400]	880±400 [550~830]	360±100 [200~540]
LS	5,240±140 [5,100~5,400]	3,900±100 [3,800~4,000]		1,030±240 [790~1,270]	540±60 [480~600]	420±80 [340~500]		370±30 [340~400]
EW	2,600±980 [1,850~4,000]	2,370±1,500 [940~4,500]	2,040	300±90 [240~430]	640±50 [580~670]	470±110 [350~620]	760	510±30 [480~550]

Table 5: Carbon concentrations in the 3 sampled groundwater and in the 6 sampled first order streams during the sampling period (Jan. 2014-Jul. 2015). HF, GS, LS and EW represent respectively high flow periods, growing season periods, late summer periods and early winter periods (Tab. S1). Numbers represent the mean±SD and the range (between square brackets).

955

	DIC$_{export}$ mmol m^{-2} d^{-1}				DOC$_{export}$ mmol m^{-2} d^{-1}				F$_{degass}$ mmol m^{-2} d^{-1}
Period	Bilos piezometer	Piezometer 2	Piezometer 3	Streams[b]	Bilos piezometer	Piezometer 2	Piezometer 3	Streams[b]	
HF	1.8±0.4	1.4±0.2	1.8±0.1	0.3±0.1	3.4±1.1	0.4±0.02	1.5±0.2	0.6±0.1	1.1±0.3
	[1.3~2.2]	[1.3~1.6]	[1.7~1.9]	[0.3~0.4]	[2.3~4.9]	[0.3~0.4]	[1.2~1.7]	[0.5~0.7]	[0.7~1.3]
GS	0.7±0.3	0.3±0.1	0.6±0.1	0.1±0.03	0.4±0.4	0.1±0.02	0.2±0.2	0.1±0.1	0.5±0.2
	[0.4~1.3]	[0.3~0.5]	[0.4~0.7]	[0.05~0.2]	[0.1~1.2]	[0.1~0.2]	[0.1~0.4]	[0.05~0.3]	[0.2~0.9]
LS	0.6±0.03	0.4±0.05		0.1±0.01	0.1±0.01	0.1±0.04		0.1±0.01	0.2±0.03
	[0.6~0.7]	[0.4~0.5]		[0.1~0.1]	[0.1~0.1]	[0.1~0.1]		[0.05~0.1]	[0.2~0.2]
EW	0.7±0.1	0.6±0.2	0.6	0.1±0.02	0.1±0.02	0.1±0.03	0.2	0.1±0.02	0.7±0.07
	[0.5~0.8]	[0.4~0.8]		[0.1~0.1]	[0.1~0.2]	[0.1~0.1]		[0.1~0.1]	[0.6~0.8]
Sampling period	0.9±0.5	0.6±0.4	1.0±0.6	0.1±0.1	0.9±0.9	0.1±0.1	0.6±0.6	0.2±0.2	0.6±0.3
	[0.4~2.2]	[0.3~1.6]	[0.4~1.9]	[0.05~0.4]	[0.06~4.9]	[0.05~0.4]	[0.2~3.0]	[0.05~0.7]	[0.2~1.3]
Mean weighted[a]	0.9±0.5				0.7±0.7				

Table 6: Export of DIC and DOC from the 3 sampled groundwater to first order streams, as well as degassing (F$_{degass}$) in first order streams during the sampling period, high flow (HF), growing season (GS), late summer (LS) and early winter (EW) periods. Numbers represent the mean±SD whereas numbers between square brackets represent the range. Here, F$_{degass}$ was calculated with the DIC data from the 3 sampled groundwaters. [a] represents the mean C export weighted by surface assuming that the Bilos piezometer is representative of wet Landes, that Piezometer 2 is representative of dry Landes and that Piezometer 3 is representative of mesophyll Landes. [b]represents C exports from first to second order streams and it have been calculated from the drainage of first order streams (m d^{-1}) and the mean concentrations of DIC/DOC in first order streams (mmol m^{-3}).

960

Figure captions

Figure 1: Map of the Leyre watershed with topography showing the location of the gauging stations (GL, PL, GAR and BR for the Grande Leyre, the Petite Leyre, the Grand Arriou and the Bourron, respectively), the Bilos site, as well as the locations of the other sampled groundwater and first order streams. Rain gauge and Eddy tower are located at the Bilos plot.

Figure 2: Seasonal variations of hydrological parameters in the Leyre watershed. (a) Discharge of the Leyre River (GL), Petite Leyre river (PL), Grand Arriou river (GAR) and Bourron river (BR) associated with water table at the Bilos site; (b) Metabolic parameters (NEE, GPP, Reco) estimated at the Bilos site; (c) Monthly precipitation (P), evapotranspiration (ETR) and groundwater storage (GWS) at the Bilos site as well as drainage (D) of first order streams. HF, GS, LS and EW represent respectively high flow, growing season, late summer, and early winter periods.

Figure 3: Monthly water mass balance at the Bilos site for the 2014-2015 period. Pearson coefficient R = 0.85, p-value < 0.001. Blue points represent months where GWS (Mar. 2014, Apr. 2014, Mar. 2015, Apr. 2015, Jun. 2015, Jul. 2015) is extremely negative (see Fig. 2c). These blue points are further away from the 1:1 Line than the other months (represented in black). The drainage of the Leyre River is delayed compared to the drainage of Bilos plot. Thus, when the loss of groundwater is extremely high (GWS negative), estimated D do not correspond exactly to measured GWS. Hence, we expected more mismatch when GWS is extremely negative.

Figure 4: Concentration of DIC and DOC in the three sampled groundwater as a function of water table depth.

Figure 5: (a) Discharge of the Leyre (GL), Petite Leyre (PL), Grand Arriou (GAR) and Bourron (BR) rivers associated with water table at the Bilos site. Temporal variations throughout the sampling period of (b) DIC in the three sampled groundwater and in the 6 sampled first order streams (medium dashed line; errors bars represent standard deviation of the 6 first order streams) and of (c) DOC in the three sampled groundwater and DOC in the 6 sampled first order streams (medium dashed line; errors bars represent standard deviation of the 6 first order streams). HF, GS, LS and EW represent respectively high flow periods, growing season periods, late summer periods and early winter periods.

Figure 6: (a) mean stock of DIC and DOC between two sampling dates in Bilos groundwater. HF, GS, LS and EW represent respectively high flow periods, growing season periods, late summer periods and early winter periods.

Figure 7: Conceptual model at the vegetation-soil-groundwater-stream interface of the Leyre catchment. OH, WT and D are organic horizon of the soil, groundwater table and drainage, respectively. Hydro-biogeochemical processes are represented in medium dash black arrows. C exports are represented in full arrows; the thickness of the arrow provides qualitative information on the flux.[DOC] and [DIC] represents the concentration of DOC and DIC in shallow groundwater, respectively. HF, GS, LS and EW represent respectively high flow periods, growing season periods, late summer periods and early winter periods.

990

Figure 1

Figure 2

995

Figure 3

Figure 4

000
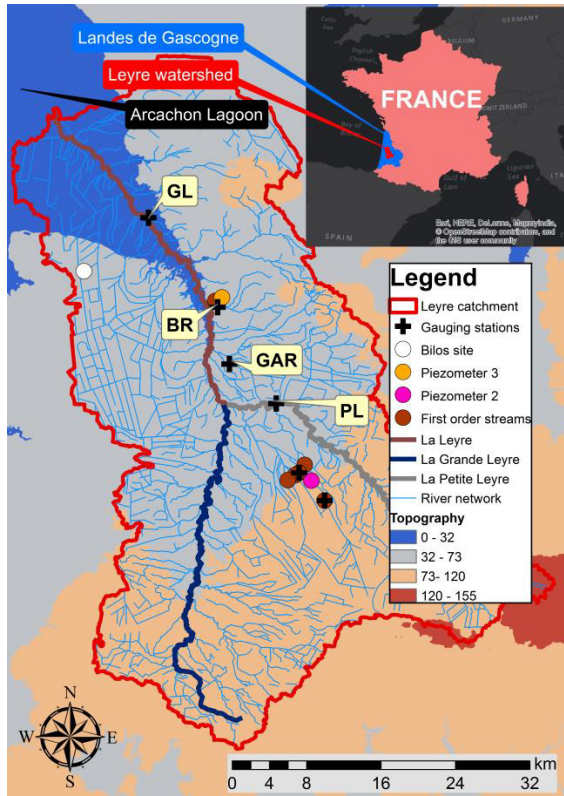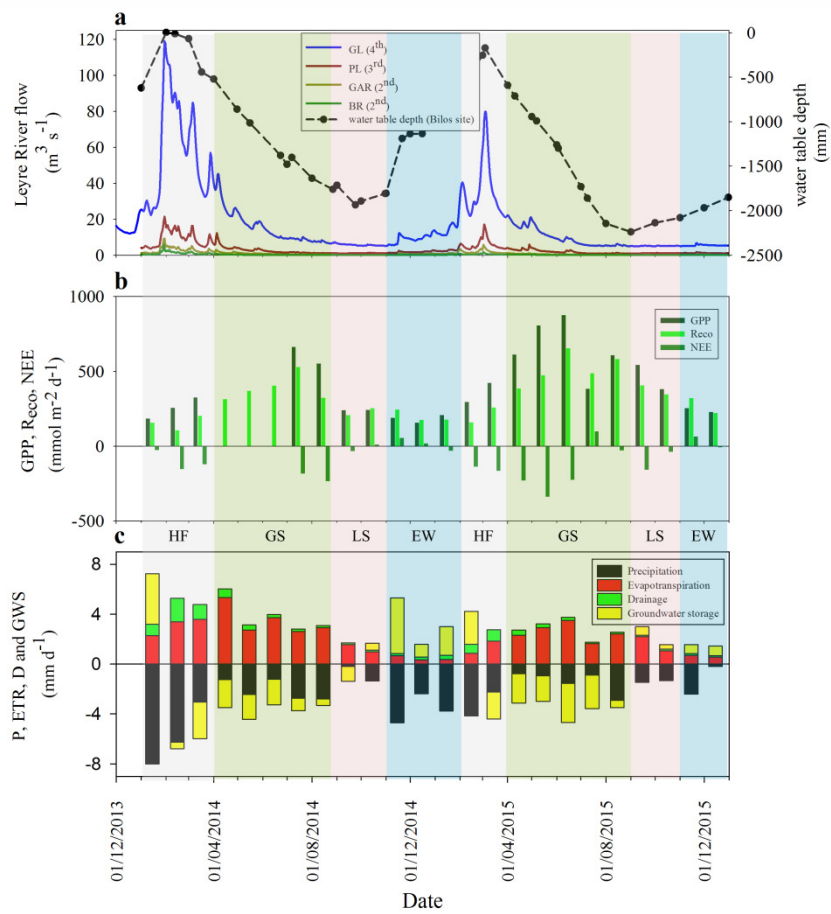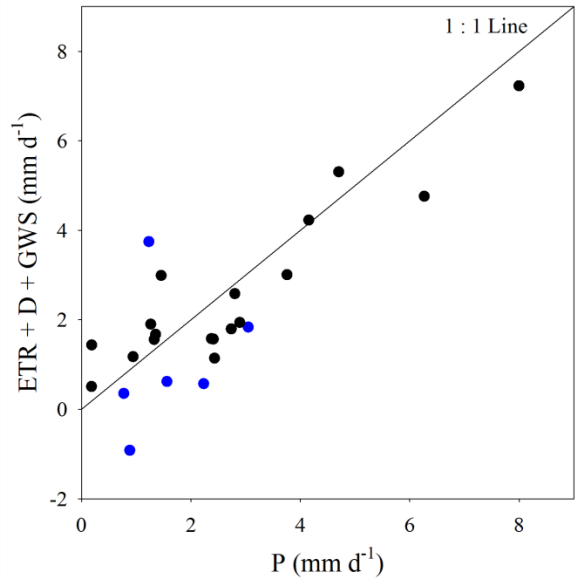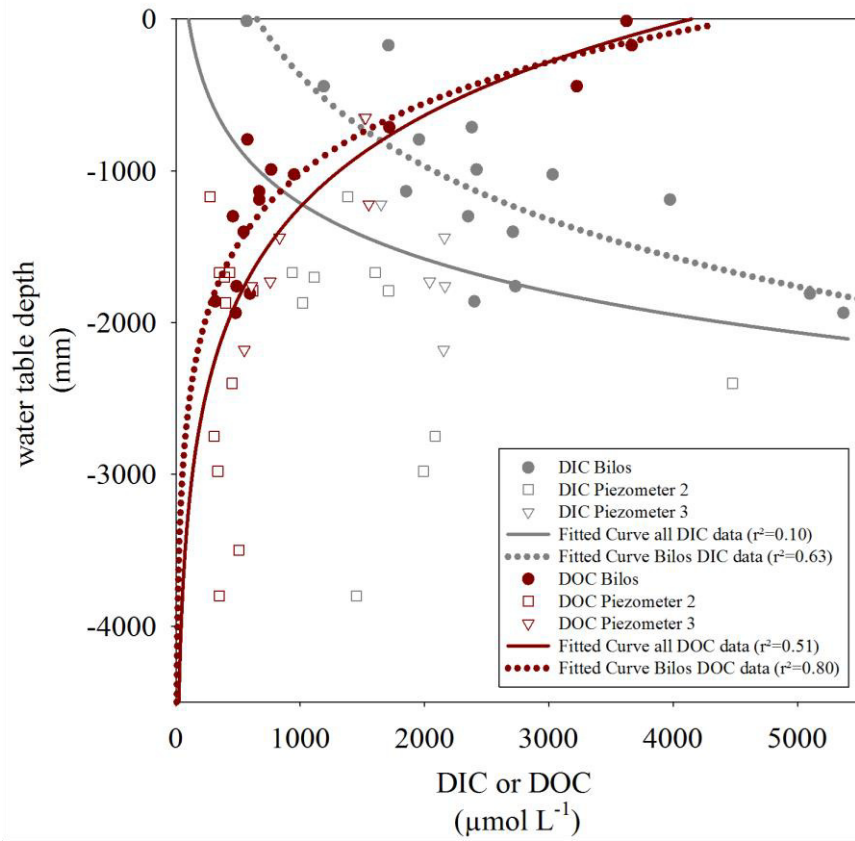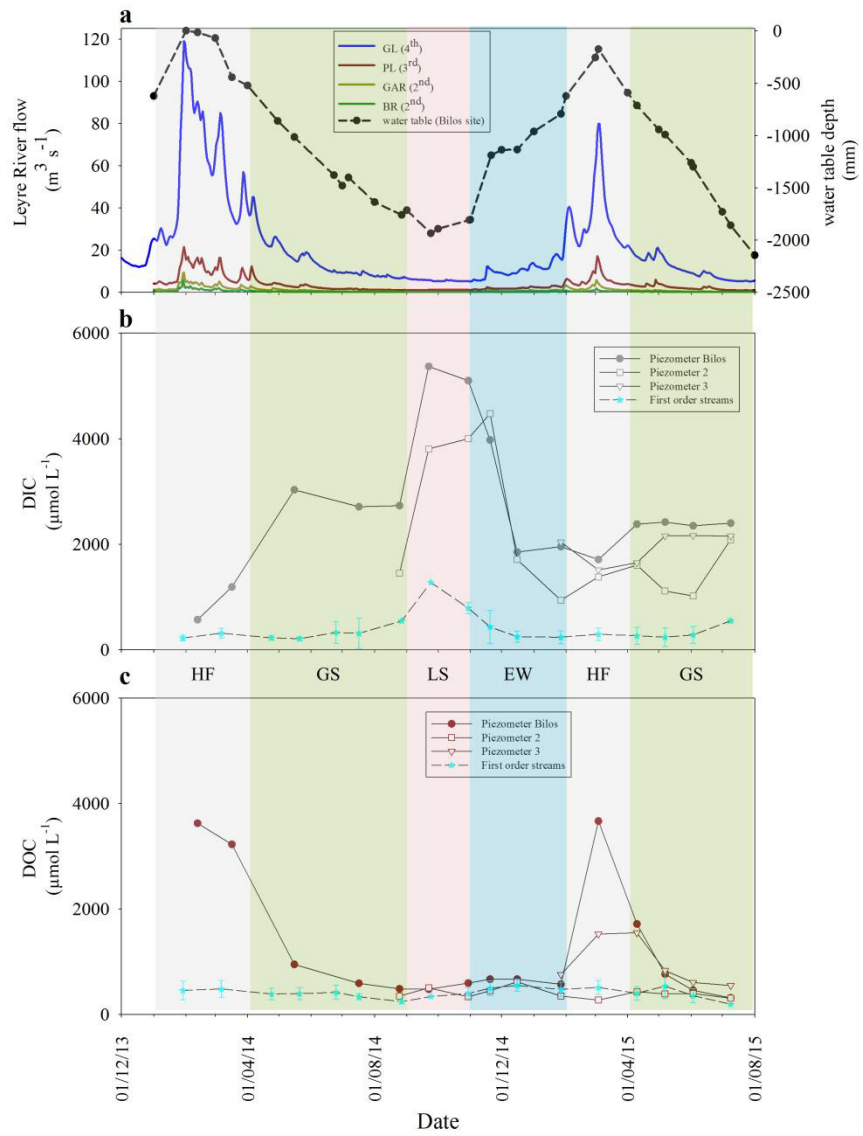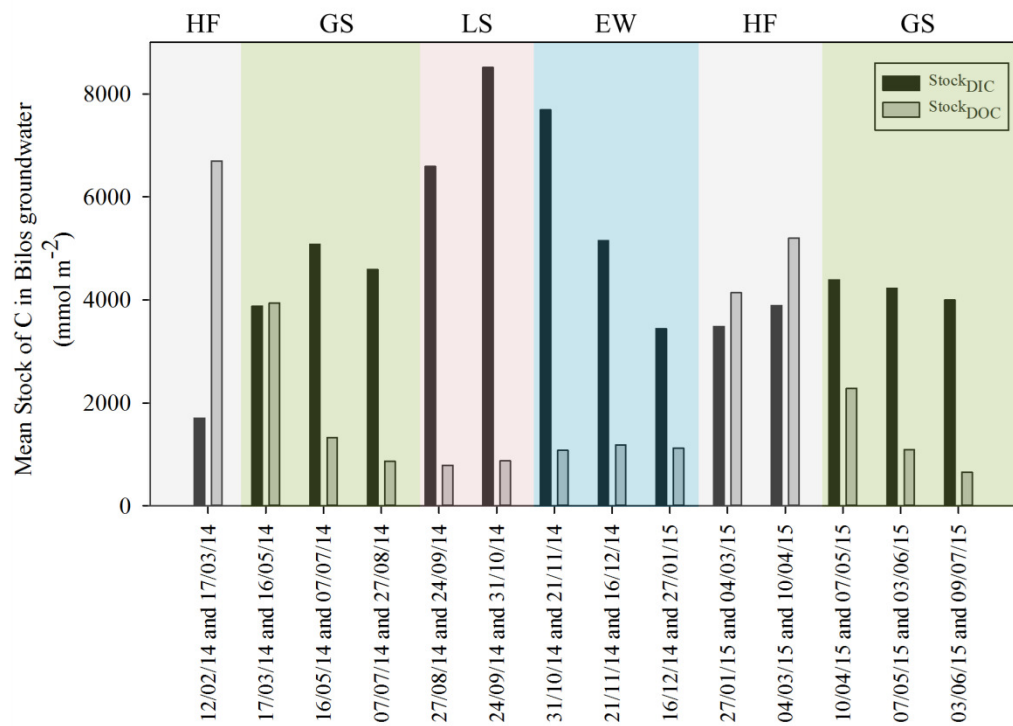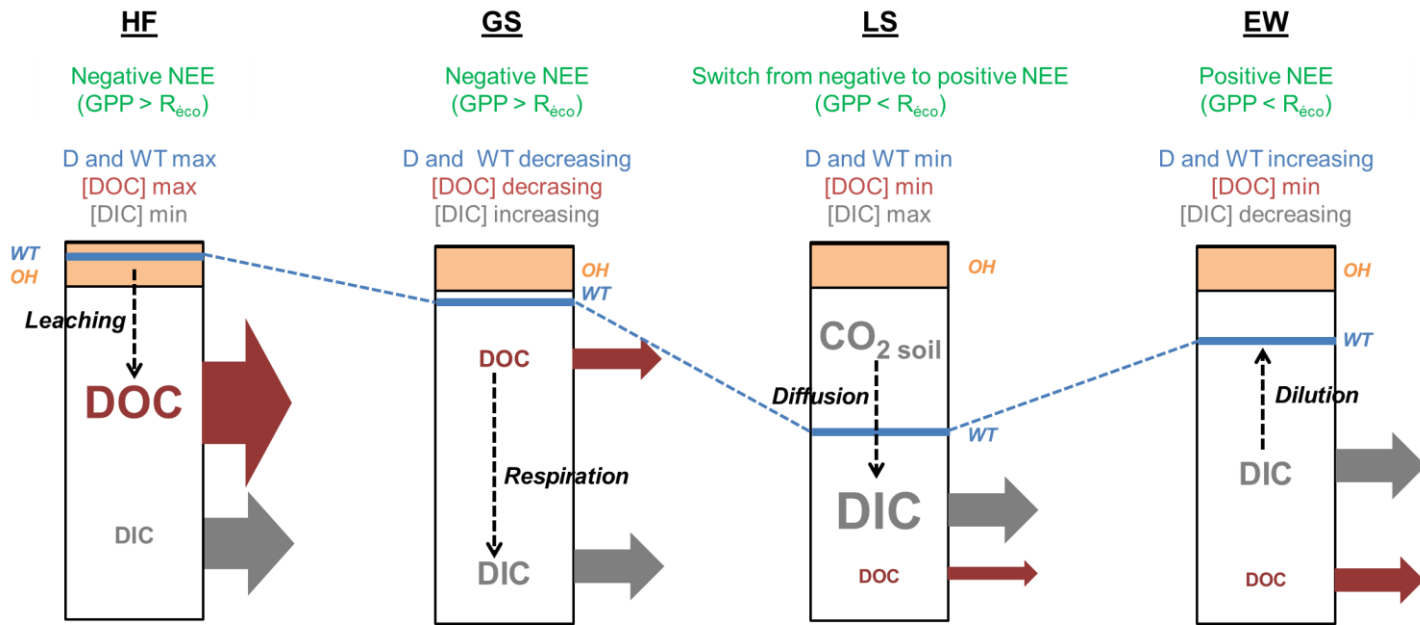
Figure 5

Figure 6

Supplementary Material

Period	Date	Groundwater			Surface water
		Piezometer Bilos	Piezometer 2	Piezometer 3	First order streams
HF	29/01/2014				X
HF	12/02/2014	X			
HF	07/03/2014				X
HF	17/03/2014	X			
GS	24/04/2014				X
GS	16/05/2014	X			
GS	21/05/2014				X
GS	25/06/2014				X
GS	17/072014	X			X
GS	27/08/2014	X	X		X
LS	24/09/2014	X	X		X
LS	31/10/2014	X	X		X
EW	21/11/2014	X	X		X
EW	16/12/2014	X	X		X
EW	27/01/2015	X	X	X	X
HF	04/03/2015	X	X	X	X
GS	10/04/2015	X	X	X	X
GS	07/05/2015	X	X	X	X
GS	03/06/2015	X	X	X	X
GS	09/07/2015	X	X	X	X

010 Table S1: Sampling dates of groundwater and surface waters. X correspond to a sampling of pCO_2, TA and DOC. HF, GS, LS and EW represent high flow, growing season, late summer and early winter periods, respectively

Period	Date	DIC_{stock} and DOC_{stock}	DIC_{export} and DOC_{export}			F_{degass}
		Piezometer Bilos	Piezometer Bilos	Piezometer 2	Piezometer 3	Streams
HF	12/02/14 and 17/03/14	X	X			X[a]
GS	17/03/14 and 16/05/14	X	X			X[b]
GS	16/05/14 and 17/07/14	X	X			X[c]
GS	17/07/14 and 27/08/14	X	X			X
LS	27/08/14 and 24/09/14	X	X	X		X
LS	24/09/14 and 31/10/14	X	X	X		X
EW	31/10/14 and 21/11/14	X	X	X		X
EW	21/11/14 and 16/12/14	X	X	X		X
EW	16/12/14 and 27/01/15	X	X	X		X
HF	27/01/15 and 04/03/15	X	X	X	X	X
HF	04/03/15 and 10/04/15	X	X	X	X	X
GS	10/04/15 and 07/05/15	X	X	X	X	X
GS	07/05/15 and 03/06/15	X	X	X	X	X
GS	03/06/15 and 09/07/15	X	X	X	X	X

Table S2: Periods of calculation for C stocks, C exports and C degassing. X corresponds to a calculation. [a, b, c] for these periods the day of sampling of surface waters do not correspond exactly to the day of sampling of groundwater (Tab. S1). C stocks in groundwater can be calculated only for Bilos plot since we do not have data about the total height of the permeable layer in the other plots. HF, GS, LS and EW represent high flow, growing season, late summer and early winter periods, respectively.